LOW CYCLE FATIGUE ASSESMENT TOOL FOR WRINKLED ENERGY PIPELINES

by

© Fahad Bakhtyar

A Thesis submitted to the

School of Graduate Studies

in partial fulfillment of the requirements for the degree of

Master of Engineering

Faculty of Engineering and Applied Science

Memorial University of Newfoundland

October, 2014

St. John's Newfoundland

ABSTRACT

The majority of energy pipeline systems are buried. They may be subject to differential ground movement which as a consequence impose axial forces and bending moments onto pipeline sections that may result in local deformation of the pipeline section such as ovalization, wrinkling and buckling. For these pipelines with local plastic damage, there exists limited knowledge and guidance on the pipe mechanical integrity and remaining low-cycle fatigue life. This uncertainty influences management considerations with respect to pipe operations, repair and intervention that have potential implications for cost and safety.

Using continuum finite element methods, a numerical simulation tool was developed to simulate the local damage, using an analogue "strip test" coupon, and assess the remaining low-cycle fatigue life response. The numerical modelling procedures were calibrated using third-party data and experimental investigations performed in this study, which is a unique contribution on this subject.

The low-cycle fatigue response was influenced by the residual strain and incremental damage associated with strain energy during a loading cycle, which was characteristic of a Coffin-Manson type power law response. The low-cycle fatigue response was also correlated with other key parameters including damage radius of curvature to pipe wall thickness ratio, imposed stroke amplitude and opening or closing mode of deformation.

Recommendations to refine the numerical modelling procedures and further establish confidence in the use of the analogue “strip test” for the assessment of low-cycle fatigue response of damaged pipelines is provided.

ACKNOWLEDGEMENTS

First of all, I would like to thank my supervisors, Dr. Shawn Kenny and Dr. Amgad A. Hussein who provided me with their consistent guidance and support throughout the research program. I would like to express my deepest gratitude to them for their assistance and strong hold on the subject matter that helped me to learn a lot.

I am very thankful to my entire research group, the WoodGroup Research Lab, and in particular to M.Eng Waqas Hanif for all the technical discussions that we held over the last year. I would also like to extend my thanks to the lab technicians David Snook, William Bidgood and Mathew Curtis for their help in fabrication and instrumentation for the experimental testing.

I would like to thank the School of Graduate Studies for providing me with the School of Graduate Studies Baseline Fellowship for most part of my program. I would like to acknowledge the Wood Group Chair in Arctic and Harsh Environments Engineering at Memorial University of Newfoundland for sponsoring the research project.

Lastly and most importantly, I owe my deepest gratitude to my loving parents and my wife, Nehreeza, for their endless support in every decision and step that I took.

Table of Contents

List of Tables

List of Figures

List of Symbols and Abbreviations

ϵ	Residual strain
α	Ramberg-Osgood coefficient
$\Delta\varepsilon_p$	Plastic strain amplitude
δe	Change in eccentricity
A	Bend angle
b	fatigue ductility exponent
e	Eccentricity
e_o	Initial eccentricity
MUN	Memorial University of Newfoundland
HCF	High Cycle Fatigue
LCF	Low Cycle Fatigue
N_s	No. of cycles to failure
R	Coupon bend radius
S	Actuator stroke
SMYS	Specified minimum yield strength
t	Coupon wall thickness
U_o	Strain energy through hysteric loop cycle
U_o/V	Strain energy density
UoA	University of Alberta

UTS	Ultimate tensile stress
V	Volume of steel material

1 INTRODUCTION

1.1 Overview

Pipelines are the most efficient way of transporting petroleum products (i.e. crude oil and natural gas) throughout the globe from the resource to the end user. In Canada the pipeline network stretches out to 830,000 km with several pipeline projects worth billions of dollars are underway in the northern and Atlantic regions. Mostly these pipeline systems are buried to mitigate load effects and damage from third-party interference and maintain mechanical integrity.

Previous studies and field observations have yielded that geotechnical movements impose large displacement and bending loads onto pipeline sections, which are caused by unstable slopes, geological voids etc. As a result of these movements buckling may be produced in the pipelines which may be global or localized, depending on the type of axial loading (Compressive or Tensile), internal pressure and/or bending. Formation of wrinkling can be triggered by the presence of geometric imperfections, which may have occurred because of manufacturing errors, corrosion, dents etc. The amplitude of localized wrinkling may increase, on continuation of loading producing regions with large strain gradients (permanent plastic deformation and material softening). Consequently pipeline operators, due to limited database on localised wrinkling, undergo remedial actions such as repair which has a potential implication on cost and safety.

Research on buried pipelines was dominated by initiation and post buckling behavioural response. Previous research produced significant findings for understanding the combination of loads, i.e. axial loads, bending loads, internal pressure, material grade and internal pressure, required to produce buckling in pipeline sections. Most substantial studies in regard to this topic have been carried out at the University of Alberta (UoA) by Mohareb et al. (1993), Yoosef-Ghodsi et al. (1995), Souza and Murray (1999), Dorey et al. (2001), Myrholm (2001), Das (2002) and Zhang (2010) where as other researcher Bouwkamp et al. 1973 and Schneider 1998 have also added significant literature in this data base. The main conclusion drawn from all of the above studies was that localised wrinkling is not always detrimental to pipeline integrity depending on pipeline ductility.

Literature available in public domain i.e. Mohareb et al. (1993), Yoosef-Ghodsi et al. (1995), Souza and Murray (1999), Dorey et al. (2001), Bouwkamp et al. (1973) and Schneider 1998 do provide understanding of the topic. However, these investigations are more focussed towards buckling initiation with limited data on post buckling response of pipelines.

Fracture in wrinkled pipelines can be categorized in two damage modes: (1) tearing failure mode and (2) low cycle fatigue (LCF) failure mode. Bouwkamp et al. (1973) and Das et al. (2002) successfully produced fractures through the tearing failure mode by continuously applying large axial loads on pipeline sections. Based on these studies, however, it was concluded that the loads required to produce such a failure are so high that they surpass the normal service conditions.

For the LCF mode, pipelines when in service undergo cyclic deformation that may be due to transient operational conditions in operating pressure and temperature (e.g. shut-in and start-up) or large deformation geotechnical load events (e.g. seismic faulting, ground subsidence, frost heave, thaw settlement and ice gouging). These cyclic deformations produce plastic strain reversals on initially damaged pipeline sections causing fracture through the LCF failure mode. Das et al. (2001), Myrholm (2001) and Zhang (2010) concluded this observation from physical testing carried out at the UoA facility. Myrholm (2001) established an experimental test known as strip test, when he observed similarities in fracture shape between a pipe wrinkle and strip specimen. Later on his work was continued by Das (2001) and during his research efforts he developed a fatigue life assessment model using the data acquired from full scale physical testing, full scale numerical modelling and experimental model testing. He concluded hysteresis loop energy to be an important damage parameter for predicting the remaining life of a pipeline that has undergone localised wrinkling. Zhang (2010) later on made an effort in developing a numerical model for the experimental model. He was able to calibrate the numerical model up to the initial bending of the strip (initial damage/ localised wrinkle). From his work he concluded that the change in bending angle during the opening and closing strokes play an important role in determining the number of cycles to failure. After these assessments, efforts have been made to establish the fatigue life of an initially damaged pipeline through experimental testing and continuum numerical modelling.

Although efforts have been made to increase the database, some key parameters have not been reported in the previous studies, which are required for development of a calibrated

numerical model. Hence to develop a fatigue life model for a wrinkled pipeline, strip tests were carried out at Memorial University of Newfoundland (MUN) to increase the database and also provide a good set of data to produce a refined numerical model. The data acquired was later on extended to develop a numerical model for pipeline steel using the data present in the available literature.

This study has thus been carried out under the consideration that it would increase the database for the experimental procedure that has been established earlier which would enable to better assess the fatigue life.

1.2 Scope and Objectives

Specifically the objective of this research effort is to achieve the following:

- To expand the knowledge base and dataset on the fatigue life of localized wrinkling in a pipeline using an analogue "strip test" physical model,
- To use the experimental dataset for calibrating the Finite Element Modelling (FEM) procedures simulating the initial damage and low-cycle fatigue life response of a strip test coupon, and
- To assess the physical and numerical simulation results with respect to the key parameters influencing the low cycle fatigue response of a damaged strip coupon

1.3 Thesis Layout

The thesis is divided into six chapters with the first two chapters focusing on scope of work and literature review respectively. The literature review focuses on existing

database of full scale modelling, experimental test modelling and numerical simulation. Current engineering practices and design codes/standards for the designing of a system under repetitive loads and fatigue life models were also discussed.

Chapters 3 and 4 are peer reviewed publications that discuss in detail numerical simulation technique and physical testing for the experimental model that was developed by earlier researchers for assessing the fatigue life of the strip specimen.

Chapter 3 focuses on the numerical simulation of the monotonic bending of the strip specimen and assessment of Bauschinger effect during the cyclic loading and unloading using the data available in public domain. A detailed model matrix was developed to expand the current database for the low cycle fatigue on the wrinkled pipelines.

Chapter 4 focusses on the need of physical testing of the experimental model based on the outcomes of chapter 3. A refined numerical model was established from the data acquired through testing however, still more efforts are required to develop a calibrated model for the assessment of fatigue life.

Chapter 5 summarizes the work done for this research and also draws the conclusive remarks that were observed during the testing. Recommendations were formulated for improvements to the physical test program and refinement of the numerical modelling procedures simulating the low-cycle fatigue response of a pipe segment with local damage. Furthermore, effectiveness of one-dimensional strip test analogue to account for other factors at full-scale (e.g. geometry, pressure, constraint) should be examined.

2 LITERATURE REVIEW

2.1 General

Failure in pipelines has always been a major concern since its practicality and low price methods have increased in the last few decades. In order to better understand the failure concept and form a set method for integrity management various codes and standards have been introduced. The codes and standards that were reviewed for this study are Det Norske Offshore Standards for Submarine Pipeline Systems (DNV, 2012) and Canadian Oil and Gas Pipeline System Code (CSA, 2010). It was found that these standards mostly followed an elastic, stress based design with either prescriptive or goal based requirements for minimum standards or recommended practice.

Ground displacement events such as long term slopes, seismic movement and ice gouging, along with operational load variation impose large loads and bending moments onto pipelines. As a consequence to these loads and bending moment pipelines may undergo localised wrinkling. Various researchers have shown that pipelines are highly ductile and may not experience a loss of mechanical integrity or product containment due to the formation of a wrinkle (Myrholm, 2001; Das, 2002 and Zhang, 2010).

Due to variation in operational loads and geotechnical movements, pipelines undergo cyclic loading and unloading which is extremely detrimental to pipelines and specifically to those pipelines which have already undergone localised wrinkling. Such pipeline segments only require a few cycles it to fracture.

Low cycle fatigue is a very well recognised concept but lack of research in this topic yields only a few guidelines in the literature. An extensive literature review was carried out to understand the low cycle fatigue (LCF) concept in metals and steel structures. The objective was to establish a method for determining the remaining life of a pipeline undergoing low cycle fatigue. In the literature review it was found that numerical simulation were only limited to full scale models and no significant efforts were put in establishing a connection between the full scale numerical model and experimental model.

The major contributions on predicting the low cycle fatigue life assessment of damaged pipeline have been carried out at the University of Alberta with the studies of Myrholm (2001), Das (2003) and Zhang (2010).

Myrholm (2001) developed an experimental model known as “Strip Test” for predicting the remaining life of a pipeline that has undergone wrinkling. In strip test a longitudinal strip of 57 mm in width and 535 mm was extracted from a pipeline and was bent around the centre as shown in Fig. 2-1.

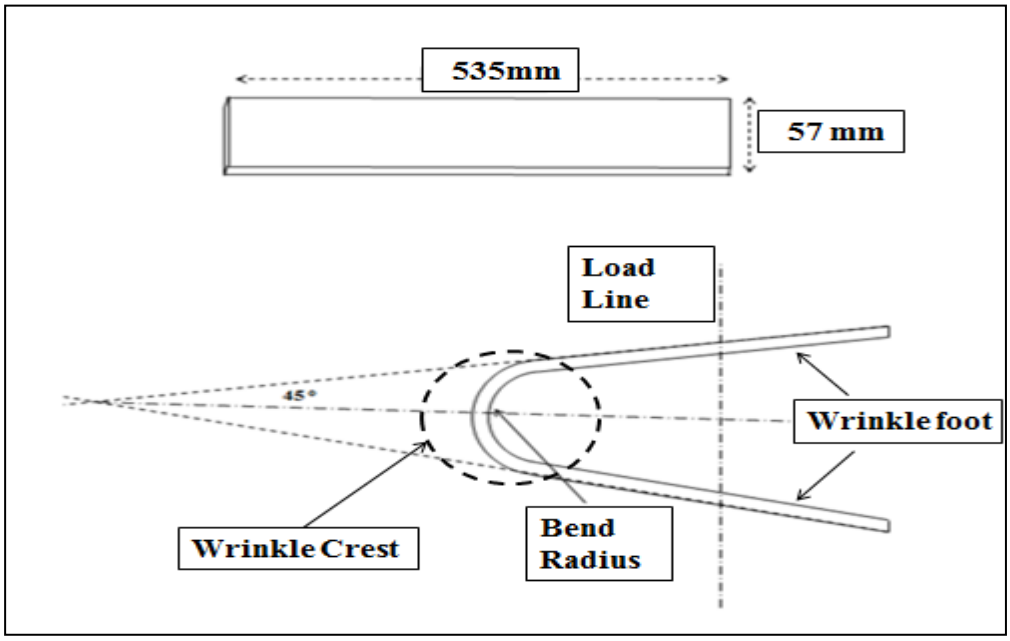

Figure 2-1: Schematic of longitudinal and bent strip

The bended strip was classified into two portions: wrinkle crest and foot as shown in Fig. 2-1. The bended strip was then subjected to displacement controlled cycles until it fractured. Similar fractures were observed at the crest of the bent strip and full-scale pipe which were subjected to low cycle as reported in Das (2003). Hence it was concluded that the experimental model was a good method for predicting the remaining life a wrinkled pipeline.

2.2 Design Standards

2.2.1 Det Norske offshore Standards for Submarine Pipeline Systems (DNV, 2012)

DNV 2012 has divided failure modes into two categories based on criticality, Serviceability limit states (SLS) and Ultimate limit state (ULS). SLS is based on different

scenarios such as dent, ovalization, ratcheting and displacement; whereas, ULS is further subcategorised into Fatigue Limit State (FLS) and Accidental Limit State (ALS) which account for accumulated cyclic and accidental loads. The scenarios considered under ULS are bursting, fatigue, fracture, collapse, propagation buckling and combined loading. Clauses D800 and D900 define fracture and fatigue criteria for designing of a pipeline system according to which fracture mechanics may be used when appropriate and the criteria shall be determined case to case, thus indicating no specific design criteria for fatigue.

2.2.2 Canadian Oil and Gas Pipeline System Code (CSA, 2010)

In section C.3.4 limit states are categorised similar to DNV i.e. Ultimate limit state and Serviceability limit state. ULS includes the parameters that are related to burst or collapse i.e. ruptures, primary loads, buckling resulting in rupture and fatigue whereas, SLS deals with parameters that affect durability of pipeline systems. Section C.6.3.3 provides detail for collapse due to external pressure, compressive strain and stress limit for axial loading, ovalization and global buckling. Section C.6.3.4 deals with fatigue and describes recognised methods for designing pipeline systems. Clause C.6.3.4.4 describes S-N curve technique for predicting life of pipeline systems while keeping in consideration, material details, construction details, state of stress and strain and surrounding environment. Clause C.6.3.4.5 states to use linear damage hypothesis (Miner's rule) for predicting cumulative damage, when stress fluctuation occur randomly. However, CSA also does not describe any detail or specific design criteria for fatigue.

Hence from the codes and standards studied during the literature review showed that these codes were more focussed towards HCF assessment of a pipeline with a little review on LCF.

2.3 Previous Studies on Localized Buckling

Bouwkamp and Stephen (1973) carried out physical testing on a 48 inch diameter X60 grade pipeline that was being used for the construction of the Alaska pipeline. The main aim of the research effort was to find local wrinkling initiation criteria and the eventual rupture of the pipeline. To be able to generate a wide set of data, different parameters were varied such as internal pressure, axial loads and pure moment (by applying lateral load). A four point bending test was carried out on the pipe which was laid out vertically on the test setup as shown in Fig. 2-2.The loading setup was kept consistent with the following pattern: pressurization, axial loading and lateral loading (for moment). Major conclusion drawn from the research were the buckle shapes (inward and outward bulge) that were dependent on internal pressure variation (i.e. zero and applied internal pressure). Another significant observation drawn was that eventual rupture was produced by the tearing failure mode. This failure was produced by very high values axial loadings which were beyond yielding limits of the pipeline and they greatly exceeded normal service condition.

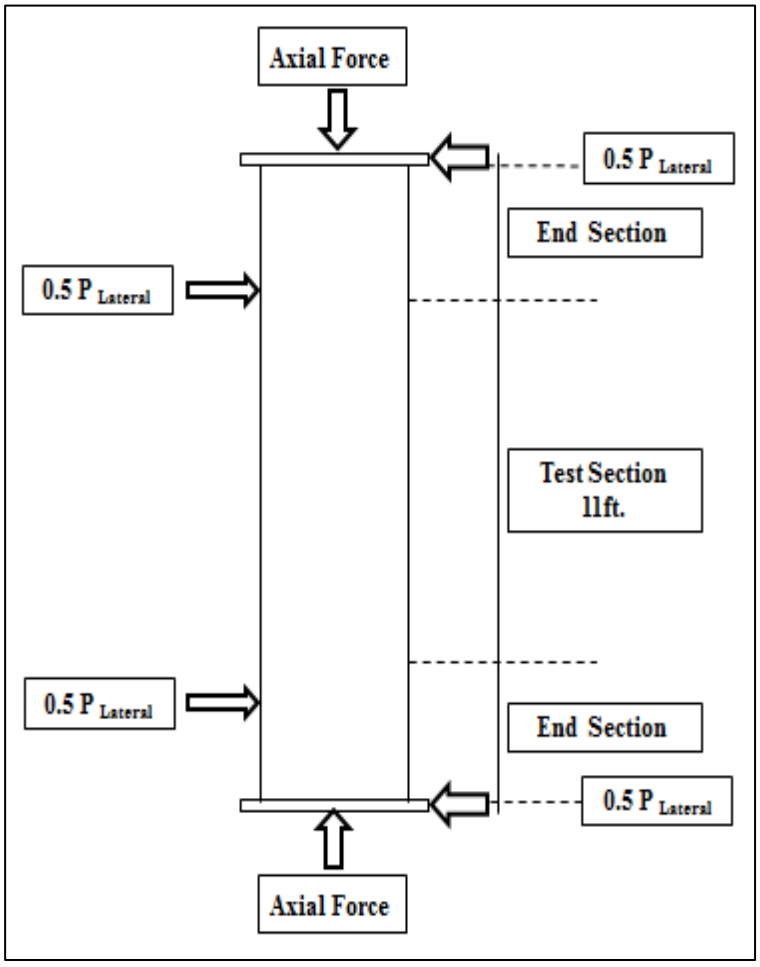

Figure 2-2: Test set-up used by Bouwkamp and Stephen (1973)

Murray (1993) carried out an analytical investigation on bending stresses in a pipeline on wrinkle bends. Using the Castigliano's theorem in conjunction with Timoshenko and Goodier (1970) stress concentration factor, he concluded that there is a large stress concentration on the inside surface of the wrinkle crest, which on pressure and temperature fluctuation may cause a fatigue problem to pipeline integrity.

Mohareb et al. (1993) carried out full scale pipe testing to investigate the limiting criteria for buckling in a pipeline. The test setup was different from Bouwkamp and Stephen

(1973), as it used rotation on the end pipes for applying a uniform moment rather than the four point beam loading scheme shown in Fig. 2-3. Conclusions from the physical tests were local buckling response was mainly dependent on initial imperfection, fabrication method, material properties and the residual stresses induced during construction of the pipeline.

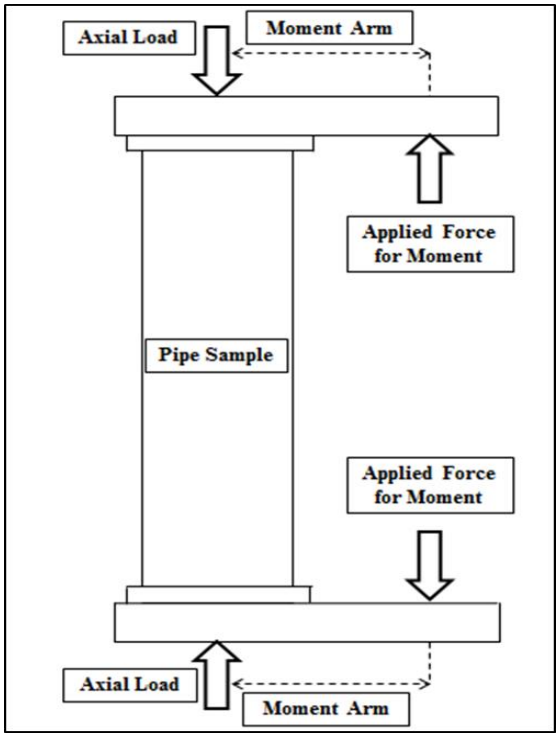

Figure 2-3: Test set-up used by Mohareb et al. (1993)

Zimmerman et al. (1995) carried out research on wrinkling capacity of a pipeline. They expressed current practices were conservative for limiting the compressive strain in a pipeline system to the curvature associated with peak moment. The research was aimed to develop a new method for predicting the allowable compressive strain in pipelines. A large scale testing programme was carried out with a non-linear finite element analysis at

the end. The result deduced from the testing were that initial imperfection were significant for predicting the initial buckling along with level of strains required to initiate it. Parametric study was carried out using the finite element model and they came up with a new critical strain (ϵ_{cr}) for pipeline design.

$$\epsilon_{cr} = 0.21\left(\frac{t}{D}\right)^{0.55} + 110\left(\frac{\sigma_\theta - 390}{E}\right)^{1.5} \qquad \text{Eq. (2.1)}$$

The hoop stress resulting from internal pressure is denoted by σ_θ, E is the elastic modulus and D/t is the diameter to thickness ratio. They recommended a 10% strain limit along the hoop direction at the crest of the wrinkle for pipeline integrity.

Yoosef-Ghodsi et al. (1995) research efforts were more inclined towards the effect of girth weld on a pipeline during localised buckling. A total of seven test specimens were tested under a similar test setup as by Mohareb et al. (1993). Axial loading and internal pressure were kept constant while curvature was increased monotonically until localised buckling was produced. It was observed, that softening of moment curvature occurred during pipeline buckling, with this slope being steeper for pipes with zero or lower internal pressure. In comparison with Mohareb et.al (1993) research it was found that initiation of wrinkling in pipes with girth weld was produced at approximately 60 percent strain levels.

Souza and Murray (1996) carried out investigation on buckling of pipelines through finite element analysis in ABAQUS. The main aim of the research effort was to develop a numerical model that could be used to assess the pre-buckling and post-buckling

behaviour of a pipeline that has undergone localised buckling. Moment curvature response in the softening zone was reliably predicted in the numerical modelling. It was observed that a sudden collapse was not produced at the wrinkle within the yielding limit of the pipeline.

Murray (1997) summarized the research carried out at UoA till mid 90's. His research effort also provided a finite element model for a pipeline on an area of non-uniform settlement. He also described the process of wrinkle formation i.e. on increasing curvature of a pipeline a point of maximum moment resistance occurs, beyond this point a decrease in moment occurs at a certain location. As a result of this decrease, assistance is provided to softening of material in the surrounding area of the point which yields to strain concentration at these points. As strain concentration continues to localise, amplification in localisation occurs at the same point resulting in formation of a wrinkle. According to him this mechanism of wrinkle formation is supported by the work carried out at UoA till mid 90's.

Dorey et al. (1999) used a similar test setup as Mohareb et al. (1993) and Yoosef-Ghodsi et al. (1995) but the pipe specimen tested had a very high D/t ratio of 93 as compared with earlier research. Pipe specimens with and without girth weld at the centre were tested during this research effort. Similar observations were observed as by Bouwkamp et al. (1973) that there are two types of bulges inward and outward depending on the inward pressure (non- pressurized and pressurized respectively). Localised wrinkling was produced at mid height or at the end of the specimen for pipes without the girth weld and

no conclusive statement was made for this inconsistency. For moment curvature during post buckling behaviour steeper slopes were observed for lower internal pressures.

2.4 Previous Research on Post Buckling Analysis

Mostly research efforts were focussed on local buckling initiation with limited detail on post-buckling effect such as low cycle fatigue (LCF) and fracture as discussed in the previous section. A significant amount of literature is available on LCF, but specific to fatigue life assessment of a wrinkled energy pipeline, it is limited to a few researchers Myrholm (2001), Das (2002) and Zhang (2010).

Myrholm (2001) carried out a physical testing on eight pipe specimens with an outside diameter of 508 mm and D/t ratio of 62 and 85. Six of the samples had a girth weld at the mid height of the pipe whereas two were plain pipes. Three different pressure ranges ($0.8P_y$, $0.4P_y$ and $0P_y$) were considered for testing and they were kept during each test. Three different temperatures (45^oC, 37^oC, 23^oC) were also considered to keep into account the temperature differential during installation and operation. Similar setup as shown in Fig. 2-3 was used, but a pivot system (rollers) was added at the top and bottom plates so the pipe sample could rotate and also allow axial forces to be transmitted completely during rotation. Sequence for applying axial load, internal pressure and curvature was kept throughout the testing with axial loading and internal pressure at the start with small alternating increases and once required levels were achieved, curvature was applied with small increments and for load cycles was curvature was removed and reapplied. Myrholm also developed an experimental model (Strip Test) as discussed

earlier for replicating the pipe wrinkle. This model was developed as full-scale pipe testing is expensive and multiple parameters could not be studied at the same instant. Longitudinal strips were extracted from a 305 mm diameter pipe that had a thickness of 6.84 mm. The strips were there then bent around the centre at two different radii (15 mm and 20 mm) for depicting different internal pressure conditions. The bent angle was kept constant at 45 degrees for both the bent radii. Two loading mounts were attached on the either end of the bent strips, which were later used to transmit load on to the crest (centre of the bent strip) of the wrinkle. The two legs of the strips are referred as the mechanical hinges or foot of the wrinkle. These mechanical hinges are similar to the plastic hinges produced on a full-scale pipe that has undergone localised wrinkling. The distance between the load line and centre of the crest during strain reversal cycle is referred as eccentricity (e) and is also the moment arm. The initial eccentricity (e_o) was set at 70 mm. The concluding remarks made by Myrholm supported the use of experimental model as an alternate to full scale model as it showed good correlation between the load vs. stroke and moment vs. stroke diagram for the above discussed cases. Two types of buckles were observed inwards and outwards as witnessed by previous researchers. Two different types of fractures were also observed; one was when the wrinkle intersected with the girth weld and the other one was when it did not. Small fractures were produced at the intersection of the girth weld in the first type and in the second type fractures were formed in the circumferential direction at the crest of the wrinkle. Both of these fractures were produced during the load cycles. It was also proposed that the limit strain at which the fracture

occurs is more applicable way for predicting the failure in a pipeline rather than using strain at which buckling initiates.

Das (2003) continued the research on pipelines with localised buckling at UoA, a total of 12 full scale tests on NPS 12 pipe specimens with yield strength of 52 ksi or 358 MPa along with 16 samples of bent strip for strip tests were carried out. The pipes had a diameter of 508 mm and two different thicknesses (6.0 mm and 8.2 mm) were used. The test setup was similar to Myrholm (2001). The maximum curvature was applied by bending of pipe, whereas the minimum curvature was generated by varying internal pressure. The cyclic loading was applied at different global curvatures and at each level three repetitive cycles were applied. The fatigue life was observed to be in between 3.5 to 12 cycles. For the strip test similar fracture was observed as in the full scale pipe as shown in Fig. 2-4. Das (2002) concluded that pipelines are highly ductile and they do not fracture under monotonically increasing loads and on cyclic loading wrinkled pipelines fail under few cycles.

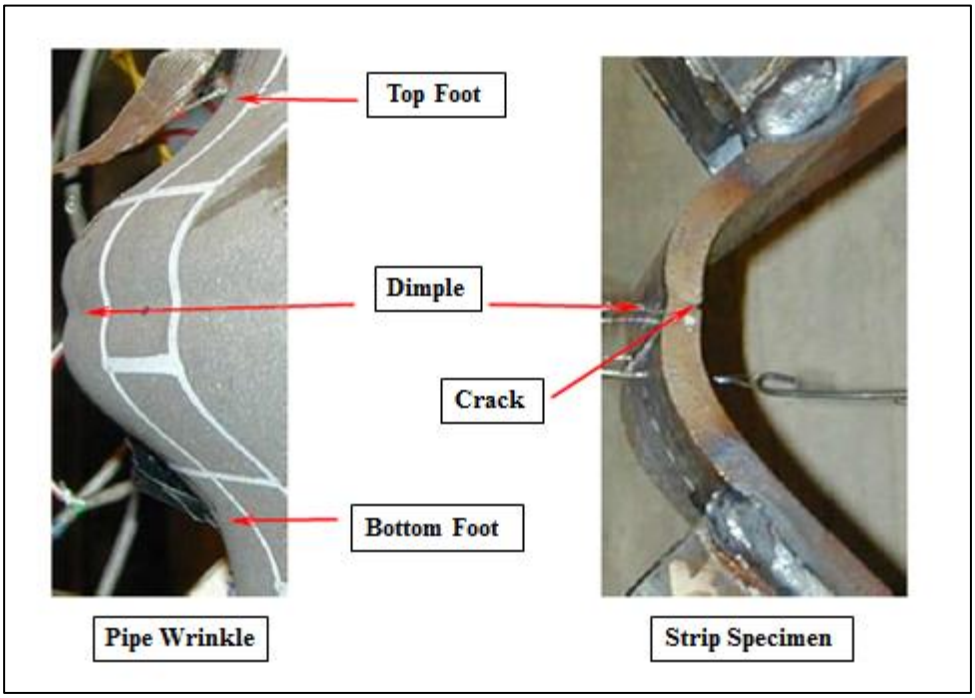

Figure 2-4: Comparison between pipe wrinkle and a strip specimen Das (2002)

Using the data gathered from full scale pipe testing and strip testing; Das (2002) developed a LCF model for winkled pipelines. He observed a relationship exists between number of cycles to initiate failure (N_s) and hysteresis loop energy (*HLE* or U_o). HLE is defined as the amount of energy absorbed per unit by the crest of the strip specimen or in other words it is the measure of damage per unit cycle.

$$N_s = A(U_o)^{-2.58} \qquad \text{Eq. (2.2)}$$

where *A* is a coefficient and it is thickness dependent. For the three thicknesses, 6.0 mm, 6.84 mm, and 8.3 mm, that were tested value of coefficient A are 1.30, 1.96 and 4.35 respectively. As reported by Das (2002), there was difficulty in calculating the HLE from

the hysteresis loop diagram and, more difficult to obtain from field measurements, so the computation of U_o was simplified

$$U_o = M_u \Delta\theta = \sigma_u Z \Delta\theta \qquad \text{Eq. (2.3)}$$

where, M_u is the ultimate moment (kN m), Z is the plastic sectional modulus (mm^3), σ_u is the ultimate stress (MPa) and $\Delta\vartheta$ is the change in rotation of the strip specimen (radian). Das (2002) concluded the model provided a conservative prediction for the remaining LCF of the test specimens.

Nazemi (2009) carried out investigations on axial loading, internal pressure and lateral loads that resulted in failure of X52 NPS 10 pipeline. Based on his experimental and numerical model he deduced that by monotonically increasing axial compression and lateral load which is applied at an offset of the longitudinal axis will produce a similar wrinkle as was produced in NPS 10 pipeline. From his testing he also concluded that X60 grade pipe with D/t 90 and higher than 90 do not fail with rupture mode whereas D/t 60 and lower will fail through rupture mode and for line pipes in between depend on the internal pressure.

Zhang (2010) continued the research work done by Das (2001) on wrinkled pipelines but hypothesized that HLE was not an effective measure for LCF assessment and prediction as it was not constant with increasing number of cycles where the hysteretic loop area decreased with increasing damage. In fatigue life assessment a parameter with constant amplitude is mostly chosen as the damage factor which HLE is not. Zhang (2010) carried

out the experimental test (strip test) on 40 samples with thicknesses of 6 mm, 8.3 mm and 11.9 mm and material grade of X65 and X60 whereas full scale testing was carried out on 6mm and 11.9 mm thick pipes. The stroke range for the strip test was selected from 12 mm to 80 mm stroke, so a wide set of data for fatigue life assessment could be generated. As a result of this stroke range the fatigue life of the samples varied from 3.25 to 616 cycles.

For the strip tests Zhang (2010) developed an empirical model that associated the fatigue damage with contributions from the monotonic bending phase and subsequent cyclic loading and unloading phase. The fatigue damage during the initial monotonic bending phase was defined as

$$D_m \approx \frac{2\left(1-\frac{\epsilon_{tr}}{\epsilon_{tf}}\right)}{\left(1+\frac{\sigma_{tf}}{\sigma_{ty}}\right)} + \left(\frac{\epsilon_{tr}}{\epsilon_{tf}}\right) \qquad \text{Eq. (2.4)}$$

where D_m is the damage accumulated during the initial (monotonic) bending of the strip specimen, ϵ_{tr} is the residual true strain; ϵ_{tf} is the static true fracture ductility of material, σ_{tf} is the true fracture stress and σ_{ty} is the true yield stress. Damage during the cyclic loading phase was defined as

$$D_c = \frac{N_{df}}{N_{vf}} \qquad \text{Eq. (2.5)}$$

where, N_{df} is the fatigue life of an actual strip (bent strip with residual strain) and N_{vf} is fatigue life of an undamaged strip.

A life based and deterioration rate-based LCF models were formulated. For the life based model, the parameters D_c and D_m were accumulated by using data accumulation rule (DAR)

$$D_c = (1 - (D_m)^{m_m})^{1/m_c} \quad \text{Eq. (2.6)}$$

where, m_m and m_c are constants. The deterioration based model was defined as

$$\frac{du}{dN_v} = \frac{du/dN_d}{D_c} \quad \text{Eq. (2.7)}$$

where du/dN_v is the deterioration rate of HLE of an undamaged strip and du/dN_d is the deterioration rate of an actual strip.

Other conclusions from the study by Das (2001) were the residual strain and R/t were influential parameters, the opening stroke was more detrimental than the closing stroke, and crack initiation life can be neglected whereas the crack propagation life should be considered for the LCF assessment. From the full scale tests, Das (2001) concluded the crack initiation was dependent on the seam weld, initiates at multiple locations both inside and outside surface and then it propagates inwards. The dependence of fracture initiation on the seam weld suggests further study on the relationship between LCF, the strip coupon tests and other factors influencing full-scale pipe response (e.g. pipe geometry, internal pressure, constraint effects) should be examined. Furthermore, Zhang (2010) observed that specimens with lower LCF remaining life was dominated by ductile

failure mode whereas specimens with higher LCF remaining life was governed by fatigue with intermediate LCF remaining life exhibiting mixed mode response.

2.5 LCF Life Prediction Model

Fatigue failure is divided into two subcategories depending on the number of cycles to failure that includes low cycle fatigue (LCF) and high cycle fatigue (HCF) response. LCF is associated with components subjected to large forces or deformations resulting in plastic stress response with failure that occurs with less than 10^3 load cycles to failure and typically characterized by a strain measure such as the Coffin-Manson relationship (Coffin, 1984, 1954; Manson, 1966, 1954). HCF is associated with loading cycles greater than 10^4 cycles to failure with low stress levels and primarily elastic response that can be evaluated using S-N curve.

Several approaches are being used in the industry to predict the damage caused by LCF. They are as follows

1. Stress or S-N Based Model
2. Strain Based Model
3. Energy Based Model

2.5.1 Stress or S-N Based Model

S-N curve plots have always been a significant approach of representing the fatigue life of a system, where S indicates the engineering stress and N is the number of cycles to failure. The S-N approach has been mostly applied to HCF systems; however attempts

have been made to establish a generic framework for use in structural engineering for HCF and LCF response (Ballio and Castiglioni, 1995, 1997). The technical approach accounts for the governing S-N curve, unified cumulative damage model and failure criterion that accounts for energy dissipation. Ballio et al. (1997) proposed a unified model (Eq. 2.8) for both HCF and LCF by replacing the stress range with effective stress range (Eq. 2.9).

$$N_f\left(\Delta S_{eff}\right)^{B_1} = B_2 \qquad \text{Eq. (2.8)}$$

$$\Delta S_{eff} = E\Delta\epsilon = \left(\frac{\Delta\delta_y}{\delta_y}\sigma_{ys}\right) \qquad \text{Eq. (2.9)}$$

where, N_f is number of cycles to failure, ΔS_{eff} is the effective stress range, $\Delta\epsilon$ is the local total strain, δ_y is the global displacement with $\Delta\delta_y$ as its range and σ_{ys} is the yield stress. B_1 and B_2 are material constant which can be determined through experimental tests. Later this model was verified by Ferreira et al. (1998) based on physical modelling studies.

2.5.2 Strain Based Model

For LCF, a strain based model is the most widely used approach to predict the remaining life of a system or component. Coffin (1954) and Manson (1954) independently developed a model on the fact that LCF is mostly due to plastic strain reversals. They

developed an equation known as Coffin-Manson equation (Eq. 2.10) using a power relationship between cycles to failure and plastic strain amplitude.

$$\frac{\Delta\epsilon^p}{2} = \epsilon_f'\left(2N_f\right)^c \qquad \text{Eq. (2.10)}$$

where $\Delta\epsilon^p$ is the plastic strain range, ϵ_f' is the fatigue ductility coefficient, N_f is the number of cycles to failure, and c is the fatigue ductility coefficient.

Keeping track of plastic strain range is difficult for engineering application, so it was proposed by Koh and Stephens (1991) to use total strain range as shown in Equation (2.11).

$$\epsilon_a = \frac{\sigma_f'}{E}\left(2N_f\right)^b + \epsilon_f'\left(2N_f\right)^c \qquad \text{Eq. (2.11)}$$

where, ϵ_a is the plastic strain range, and *b* and *c* are empirical coefficients. Based on the above equation 2.11, it was concluded that for small amplitudes the curve approaches elastic strain fatigue life (HCF) and for large strain amplitudes the curve approaches plastic strain fatigue life (LCF).

2.5.3 Energy Based Model

For energy based models the energy dissipated during plastic deformation is taken in account as the damage parameter. Feltner and Morrow (1961) made the initial attempt for this model when they tried to measure the plastic strain hysteresis energy and correlate it with the plastic strain fatigue fracture. The assumption of using the static true stress curve

to evaluate the plastic strain hysteresis for fatigue behaviour was not completely effective. This model was later classified into three different categories depending on the type energy that was being selected as the damage parameter by Ellyin (1997). The classifications were defined as

1. Hysteresis Energy Based Model
2. Plastic Strain Energy Based Model
3. Total Strain Energy Based Model

Efforts have been made in developing each of the above models since then. Das (2002) developed a fatigue model using the hysteresis based approach and it has been discussed earlier. An example of plastic strain energy model was given by Lefebvre and Ellyin (1984) whereas for total strain energy based model Chen (2004) developed a model using the plastic strain energy as well as total strain energy as damage parameters.

3 DEVELOPMENT OF A FATIGUE LIFE ASSESMENT TOOL FOR PIPELINES WITH LOCAL WRINKLES

This peer reviewed paper has been published in the proceedings of International Conference on Ocean, Offshore and Arctic Engineering (OMAE 2013-10556, Nantes, France). This paper was a collaborative effort that included myself and Dr. Shawn Kenny. As the primary author, I was responsible for developing and calibrating the numerical modelling procedures, conducting the data analysis and synthesizing the results within this paper. Dr. Shawn Kenny was responsible for providing supervision and guidance during this study and editorial comments in the preparation of this paper.

Authors: Fahad Bakhtyar and Shawn Kenny

3.1 Abstract

Pipelines may be subject to ground movement events or external interference that imposes axial and moment loading into the pipeline. This system demand may cause localized deformation mechanisms to develop, that may be observed as local wrinkling or buckling of the pipe wall. The local buckle amplitude may increase with continued external loading and may fracture due to low cycle fatigue failure caused by operational conditions.

There exists limited data and engineering guidance on the mechanical performance of energy pipelines with a local wrinkle or buckle. The literature suggests the fatigue service life can be significantly reduced by the presence of local wall deformation mechanisms.

In this study, continuum numerical modelling procedures are developed to assess the influence of pipeline damage in the form of a local wrinkle or buckle on the low-cycle fatigue life. The simulation tool is calibrated from the available literature and a parametric study is conducted to examine the influence of wrinkle bend radius, pipe wall thickness, cyclic displacement amplitude, material grade and constitutive models on the pipe mechanical performance.

3.2 Introduction

Pipelines are used as main mode of transporting petroleum products within North America. These pipelines are the most efficient way for delivering of crude oil, natural gas etc. at various facilities throughout the world offshore and onshore as well. Buried pipelines may be subjected to subsurface geotechnical movements that may impose large displacements and bending loads on these pipelines. This may result in causing localized curvature in the pipe wall, which can be attributed to localize wrinkling with large strain gradient across the damaged region (Jayadevan et. al (2004), Bai et. al (2008), Mahdavi et. al (2010)).

Once this wrinkle is formed, it may start to grow further if the pipeline is subjected to monotonically increasing load. If the wrinkle is subjected to subsequent cyclic loads, this may result in cyclic plastic strain reversals leading to void coalescence at strain concentration point that may ultimately lead to fracture in the wrinkled region (Das et. al (2003)). Due to uncertainty on the pipeline mechanical response, in the region of the local buckle, to additional external loading and fatigue life estimates, pipeline operators invoke

management practices that promote integrity and may include maintenance, intervention and repair (Scotberg et.al (1992), Michailides et. al (1998))

Recent studies on the fatigue life performance of pipeline with local wrinkle indicate the pipeline may fail when subject to a low number of load cycles (Das (2003), Zhang (2010)). Low cycle fatigue (LCF) is associated with high amplitude, low frequency loading condition that results in localized plastic strain with subsequent cyclic loads, typically in the elastic region, that lead to failure. The key issues with LCF assessment are the approaches which have been generally more conservative where the engineering tools are more complex than traditional fatigue assessment model for high cycle events, due to the nature of performance criteria (i.e. strain versus stress based) and material performance (e.g. degradation or damage models, global and local plastic behaviour). Characteristics of the hysteresis cycle (e.g. energy) and material performance (e.g. softening or degradation) may be significant.

Although a significant body of literature exists in the field of low-cycle fatigue (e.g. (Yao et. al (1961), Junak et. al (2011), Halford (1986), Bruton et. al (2005), Xue (2008)), there exists limited guidance on the fatigue life performance of energy pipelines with local damage due to wrinkling or buckling (Das et. al (2003), Zhang (2010), Myrholm (2001), Das et. al (2008)). The key technical gaps include development of comprehensive physical database integrating stress-strain relationships, mechanical response and hysteretic behaviour, validation of numerical simulation tools to predict the LCF of

wrinkled pipelines and advancement of robust criteria defining mechanical performance limits for LCF life associated with wrinkled pipelines.

In this study numerical modelling procedures, using ABAQUS v.6.10-2, were developed to evaluate the hysteretic response of a pipe coupon with an initial bend radius subject to cyclic loading event. The simulation tool was developed and calibrated based on experimental tests available in the public domain literature (Das (2003), Zhang (2010), and Myrholm (2001)). The pipe coupon simulated the initial plastic strain state of a full scale pipe that developed a local wrinkle. The coupon was subject to cyclic loads in order to examine the influence of wrinkle bend radius, pipe wall thickness, cyclic displacement amplitude, material grade and constitutive models on the pipe mechanical behaviour and hysteric response. These investigations will provide a basis and framework to develop a numerical tool that can help in predicting and assessing the remaining life of wrinkled pipe subject to cyclic load events.

3.3 Nomenclature

ϵ	axial strain
R	coupon bend radius
t	coupon wall thickness
SMYS	specified minimum yield strength (MPa)
α	Ramberg-Osgood coefficient
N	Ramberg-Osgood exponent

3.4 Experimental Procedures

The experimental procedure carried out in the literature (Das (2003), Zhang (2010), Myrholm (2001)) is briefly described in this section. Longitudinal strips having dimensions 535 mm x 57 mm were cut from X52 with wall thicknesses of 6mm and 8.3 mm (Das (2003)), X65 with wall thicknesses of 6mm and 8.3mm and X60 with a wall thickness of 11.9 mm (Zhang (2010)). Material properties for the above grades are defined in the Table 3-1 & 3-2.

Thickness (mm)	6	8.3
Modulus of elasticity (GPa)	202	211
Proportional limit (MPa)	314	378
Static Yield Stress (MPa)	460	479
Static Ultimate Stress (MPa)	563	546

Table 3-1: Material properties as in literature (Das (2003))

Thickness (mm)	6	8.3	11.9
Modulus of elasticity (GPa)	206.3	207.4	193.5
Proportional limit (MPa)	287.5	222	226
Static Yield Stress (MPa)	497	469	507
Static Ultimate Stress (MPa)	552	556	543

Table 3-2 : Material Properties as in literature (Zhang (2010))

A specimen width of 57 mm was selected to minimize the influence of circumferential pipe wall curvature. The coupon length was governed by the bend arc length representing the local wrinkle and tangent length required to accommodate the loading mounts attached for the target range of initial load eccentricity values (Das et. al (2003), Zhang (2010)).

The straight coupon strip was bent at mid-length by using a guiding rod and a driving wheel. The strip was fixed at one end by a clamp where a driving rod, which was free to revolve about its own axis, was rotated about the axis of a guiding rod by a desired angle (45^o). The radius of the bend is subjected to the radius of guiding rod. The bend radius was set equal to either 15 mm or 20 mm.

The bend radius was selected to represent field conditions of the local buckling event with respect to the wrinkle geometry (i.e. sharp or blunt curvature) and effects of internal

pressure conditions (i.e. low and high) on the wrinkle curvature (Das (2003)). A typical bent coupon representing the pipeline wrinkle is shown in Fig. 3-1

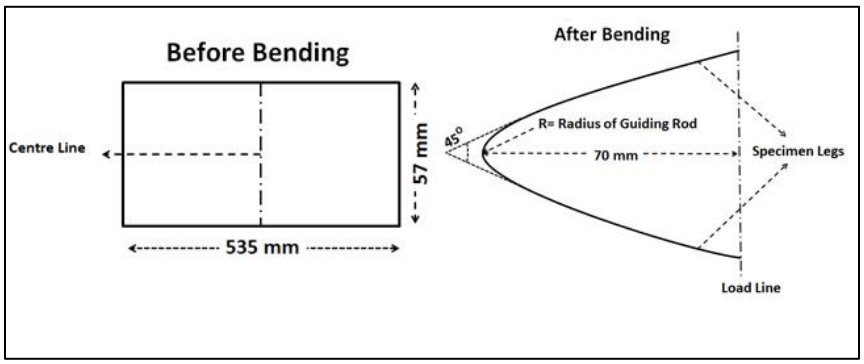

Figure 3-1: Specimen dimensions before and after bending application

After the coupon was bent into a radius of curvature, the two loading mounts were welded onto the support legs of the coupon and the loading mounts were connected to the materials testing system (MTS1000) through hydraulic grips. The coupon was subject to flexural loads by transferring the axial stroke of the MTS machine to rotation through hinges attached to the loading mounts. Cyclic loads were applied to the coupon through displacement control of the actuator stroke. This cyclic loading produced strain reversals that eventually lead to the strip specimen fracture at the crest. The experimental procedure is described in more detail in literature (Das (2003), Zhang (2010), Myrholm (2001)).

3.5 Numerical Modelling Procedures

A numerical model was developed to simulate the experimental procedures described in the preceding section (Das (2003), Zhang (2010)). The test X52-T9-A45-R20-S50 was used as the baseline calibration dataset. The symbolic test description was defined as

grade in Imperial units (X52), wall thickness in millimetres (T9), bend angle in degrees (A45), bend radius in millimetres (R20) and full actuator stroke amplitude for the compression and tension cycle in millimetres (S50).Wall thickness of 8.3 mm will be referred as T9 and similarly wall thickness of 11.9 mm as T12.

The primary objective was to develop a calibrated numerical tool that can predict the mechanical response and low cycle fatigue performance of wrinkled pipeline segments. The modelling procedures defined two stages including (1) monotonic loading of the strip specimen for producing the coupon with a target bend radius, and (2) cycling loading to investigate the mechanical response and fatigue performance.

Reduced integration shell elements (S4R) were used for the strip specimen whereas the fixed rod and the guide rod were modelled as rigid bodies. S4R elements were used for computational performance characteristics to handle large strain and reduce solution time (ABAQUS V 6.9). The deformation in the fixed rod and drive wheel were quite small as compared to those in the strip specimen so they were considered as rigid bodies. The contact properties between the strip specimen, the guide rod and fixed rod were obtained from available literature (Zhang (2010)). On the basis of applied load on the strip specimen during the bending stage it was observed that drive wheel exerted negligible load in the tangential direction so a friction coefficient of zero was given between the strip and drive wheel whereas 0.6 friction coefficient was given to the surfaces between the guide rod and strip specimen (Zhang (2010)). A mesh sensitivity study was conducted for the strip bending process that examined mechanical behaviour and residual strain

patterns. The Ramberg-Osgood relationship was used to generate discrete values of stress and strain for characterizing the material behaviour of X52 and X65 grade pipe. In the numerical modelling procedures, the stress-strain relationship was defined through piecewise representation based on these discrete values where the constitutive model was represented by J_2 flow theory of plasticity with von Mises yield criterion.

For the monotonic loading stage, one end of the coupon strip was encastered and the other end was set free to bend under the influence of driving wheel. The initial boundary conditions are illustrated in Fig. 3-2. Once the initial boundary conditions were established, the rigid drive wheel was rotated about guiding rod's axis. The guiding rod, having a radius of 20mm, was tied to a reference point, which was encastered in order to impose fixed boundary conditions in all 6 DOF. The driving wheel was then given a rotation of $180° - \theta$ (45° for this calibration case) to cause the specimen to bend. The bending stages are illustrated in Fig. 3-3.

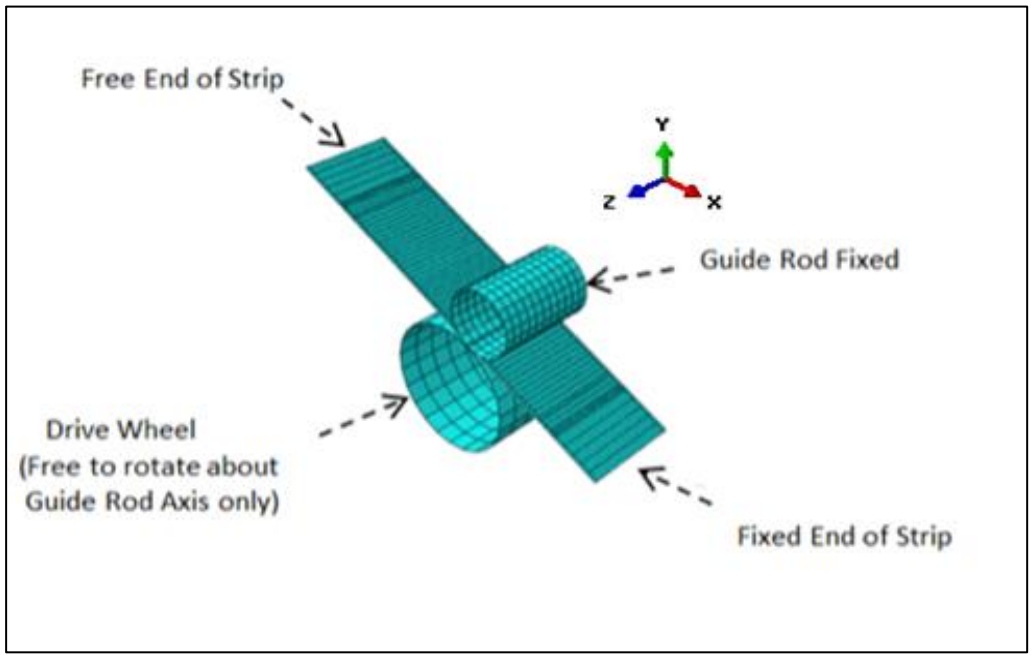

Figure 3-2: Initial boundary conditions of straight pipe strip specimen

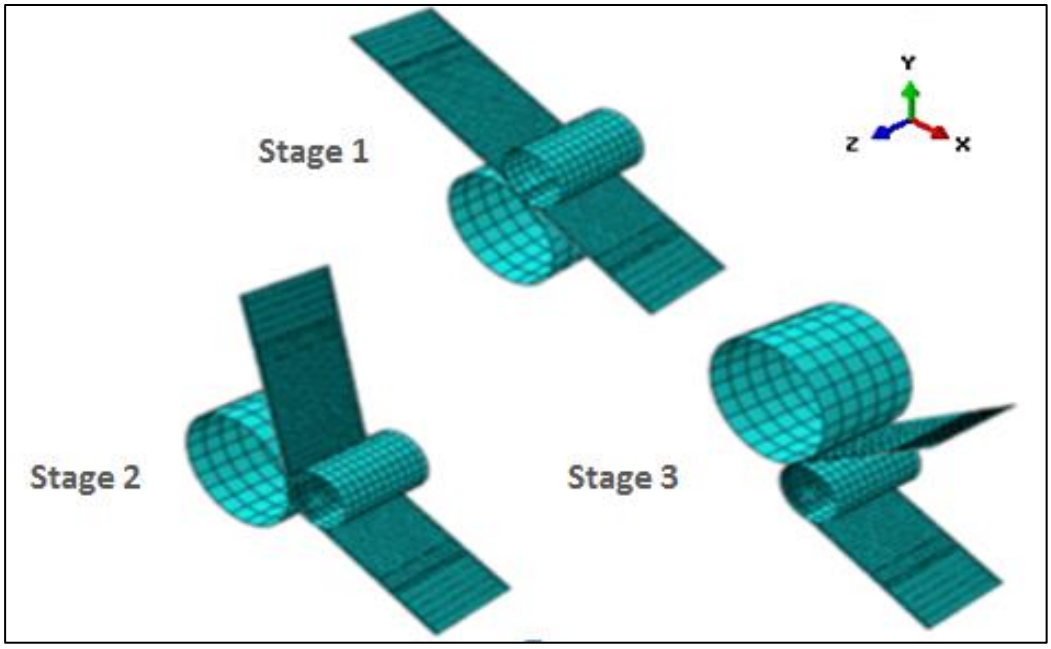

Figure 3-3: Bending stages to produce coupon

After initial bending was achieved, the specimen was subjected to cyclic loading in order to simulate field conditions. As discussed in the literature (Das et. al) initial eccentricity was set to 70 mm from the centre of the wrinkle. Taking advantage of simulation capabilities to model the imposed displacement boundary conditions, associated with the actuator stroke, the tangent length of the coupon was reduced to 240 mm. The remaining tangent length of the coupon strip does not influence the mechanical response near the bend radius (Das (2003), Zhang (2010)). This also reduced the solution run times. The principal regions of interest for the numerical simulation are the bend radius and the line of action defining the actuator stroke. The actuator stroke was imposed by defining the amplitude for the boundary condition in the y direction on the load line and changing the boundary conditions for the fixed end of the strip as illustrated in Fig. 3-4.

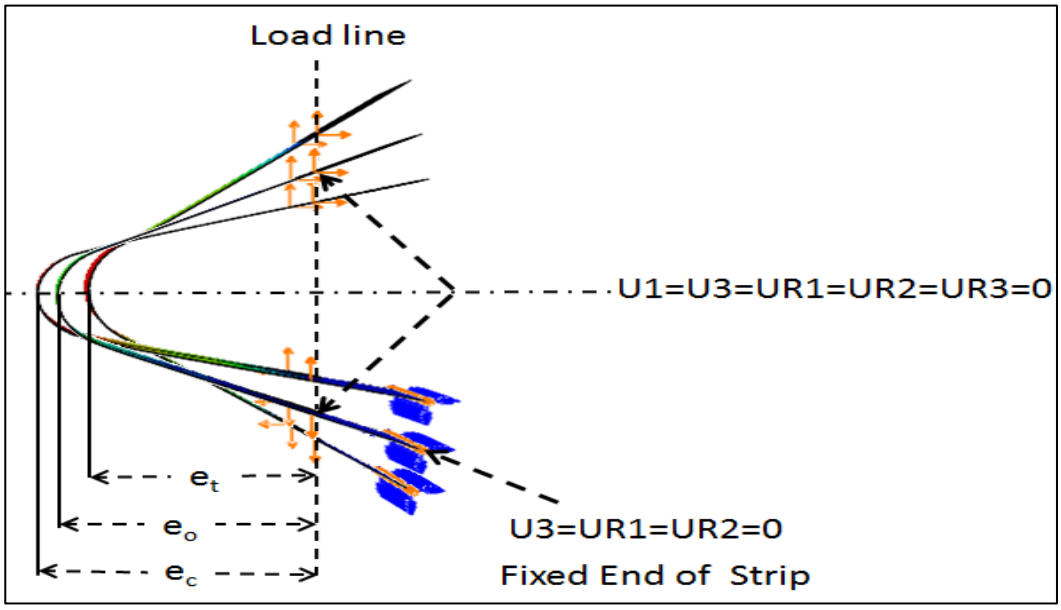

Figure 3-4: Boundary Condition for cyclic loading

The maximum stroke change of 50 mm (± 25 mm) was applied in direction of load line as given in Fig. 3-4. Due to lack of reported information on the constitutive parameters, in particular strain hardening and kinematic properties, and damage parameters, the specimen was subjected to one cycle where the load cycle response was captured and compared with available results (Das (2003)).

3.6 Residual Strain due to Bending

The coupon residual strain along the width of the strip specimen at the centre line after the monotonic loading stage was examined where the finite element predictions were compared with analytical solutions and experimental test data. The residual strain due to bending can be estimated by:

$$\epsilon = \frac{1}{\left(1+\frac{2R}{t}\right)} \qquad \text{Eq. (3.1)}$$

The strain due to bend radius (curvature) is based on idealizations formulated in beam theory (e.g. plane sections remain plane, no distortion of the cross-section) and the material behaviour is elastic, perfectly plastic.

As shown in (Fig. 3-5), the predicted residual strain based on finite element simulations, for three coupon wall thicknesses (6 mm, 9 mm and 12 mm) exhibits excellent correspondence with experimental test data in literature (Das (2003), Zhang (2010)) and analytical solutions (Eq.3.1). The residual strain decreases with increasing R/t where the analytical solution diverges at lower R/t ratios due to through thickness plastic material response. Further details of the analysis are presented in Annex A, where the residual strains for different material grades (X52 and X65) do not show any significant differences, which is consistent with other data (Zhang (2010)).

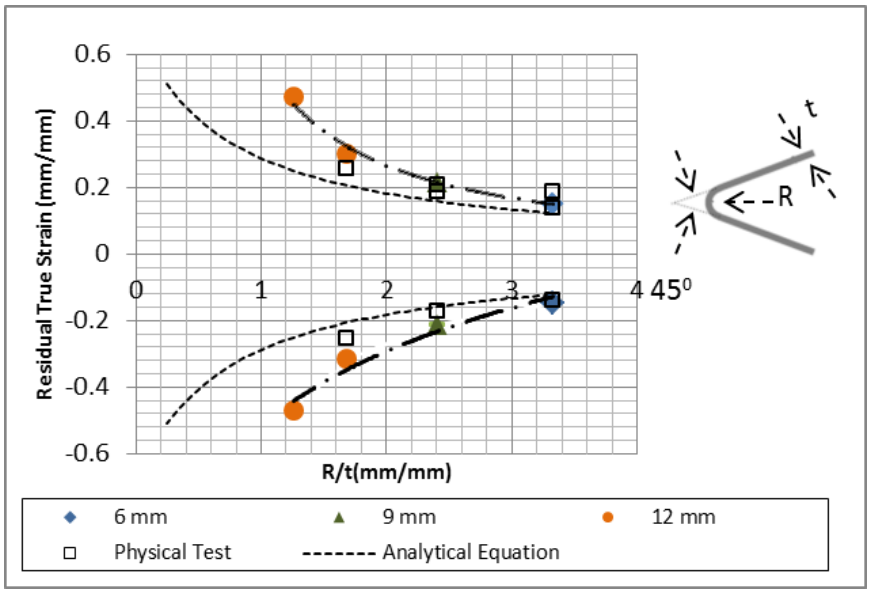

Figure 3-5: Variation of residual true strain with R/t ratio

These observations are further illustrated in Fig. 3-6 along the width of the strip specimen i.e. 57 mm at the centre line. The residual strain magnitude increases with wall thickness and is constant value along the width of the strip.

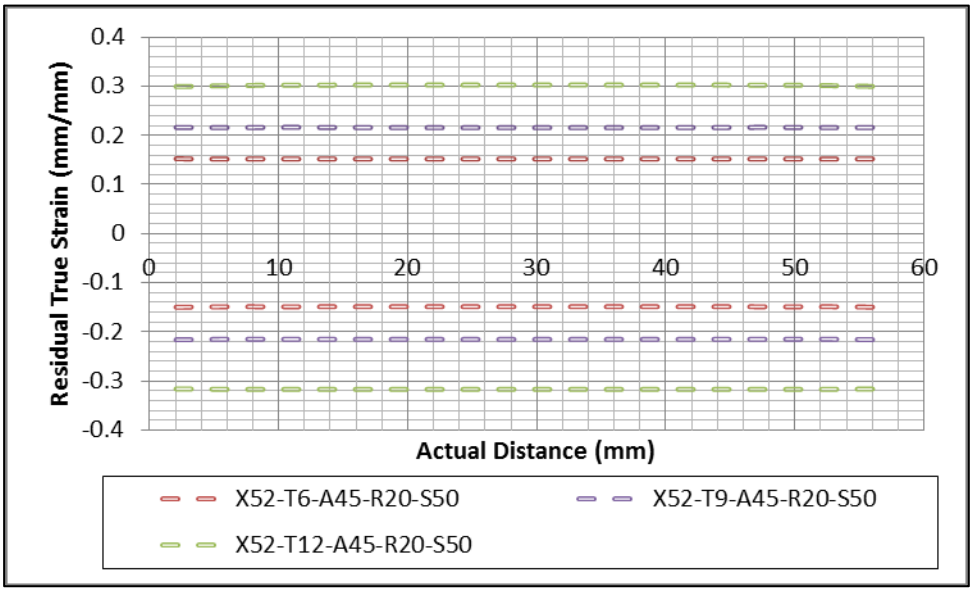

Figure 3-6: Residual true strain on the extreme fibers for the intrados and extrados

Whereas for the residual stresses it was found that the von Mises at the outer surface were lower in magnitude than those at the inner surface. Trends at both the surfaces were found to be similar. Maximum stresses were found just near the edges of the coupon strip. No significant changes were observed at the centre of the strip and this could be observed from Fig. 3-7.

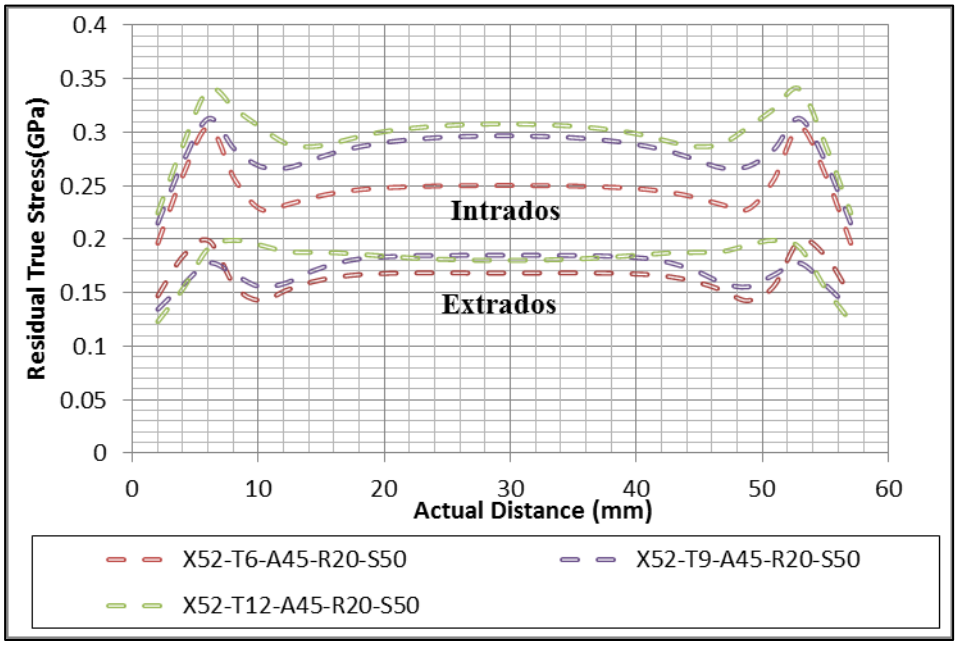

Figure 3-7: Residual true stress on the extreme fibers for the intrados and extrados

3.7 Hysteresis and Constitutive Modelling

The coupon strip with X52 Grade, bend radius of 20 mm, wall thickness of 8.3mm was subjected to a single load cycle (tension and compression) with a stroke of ±25 mm. The objective was to compare the finite element predictions, based on the numerical modelling procedures developed in this study, with third-party experimental test data provided in literature (Das (2003)) which provides a load hysteresis for the same strip specimen. Details on the constitutive parameters and stress-strain relationship, however, were not reported. In this study, it was assumed the X52 grade material could be defined with a specified minimum yield stress of 358 MPa, an ultimate tensile strength of 455 MPa, elastic modulus of 205 GPa, poisson ratio of 0.3 and Ramberg-Osgood coefficients of 1.86 and 17.99, for the yield offset and strain hardening exponent coefficients,

respectively. The constitutive model was defined using J_2 classical metal plasticity with isotropic hardening, associated flow rule with yield defined by the von Mises criterion. The use of an isotropic hardening model is consistent with other studies (Das (2003), Zhang (2010)).

A comparison of the hysteresis curve for a single load cycle as predicted by the finite element modelling procedures, developed in this study, with the experimental test data set, conducted by Das (2003), is shown in Fig. 3-8.

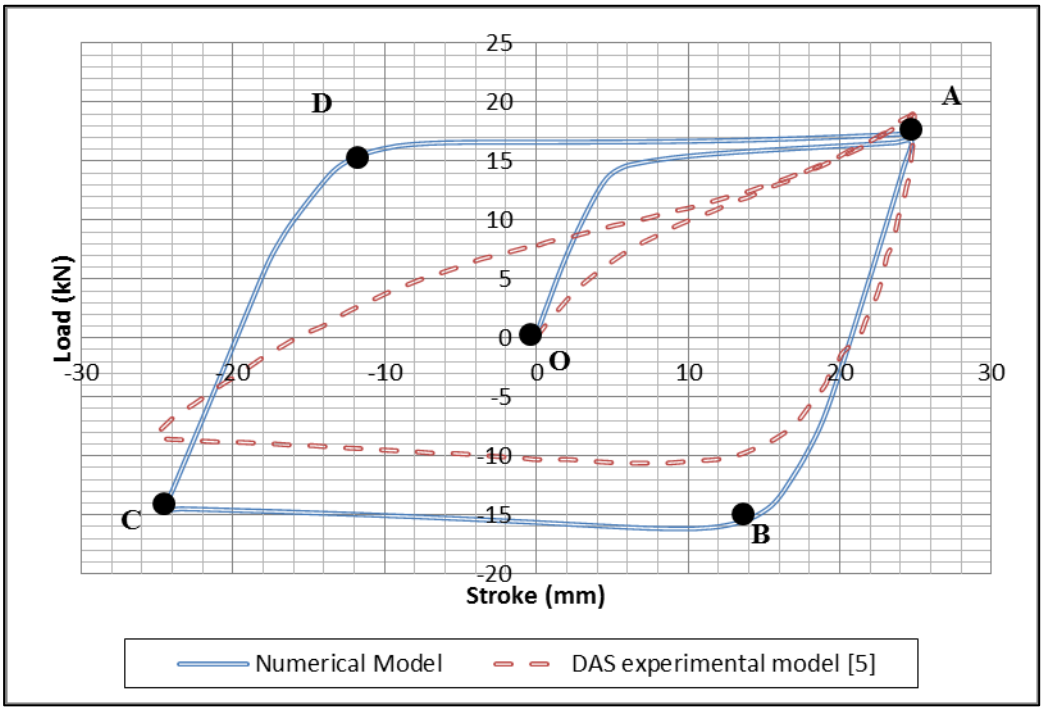

Figure 3-8: Comparison of load hysteresis loop of strip specimen for first cycle

Discrepancies between the numerical simulations and experimental tests were attributed to the boundary conditions associated with the application of the actuator stroke. The initial load step (segment OA) represents the opening mode (i.e. tension with increasing

bend angle) where the FE predictions and experimental test have the same peak value. On the unloading step (segment AB), the elastic characteristics are consistent and the FE simulation exhibits the same behaviour for all loading sequences (segments OA, AB and CD). The peak compressive load occurs at point B where differences in the compression yield response (segment BC), between the numerical simulation and experimental test, suggest Bauschinger effects may play a role such that the FE procedures do not account for kinematic hardening. However, as discussed in more detail later within this subsection, further numerical investigations using a kinematic hardening model does not support this hypothesis.

It is believed the discrepancies are due to differences in the kinematic boundary conditions for the coupon sample when imposing the actuator stroke. This statement is supported through examination of the load eccentricity being applied to the coupon (Fig. 3-9). Although the stroke range of ±25 mm is consistent for both models, the experimental tests have a significantly greater load eccentricity. The FE simulations predicted a load eccentricity of 62 mm in tension (e_t) and 76 mm in compression (e_c), whereas the experimental tests measured 40 mm and 90 mm, respectively. This influenced the moment imposed at the apex of the bend radius and affected the hysteric behaviour (Fig. 3-10).

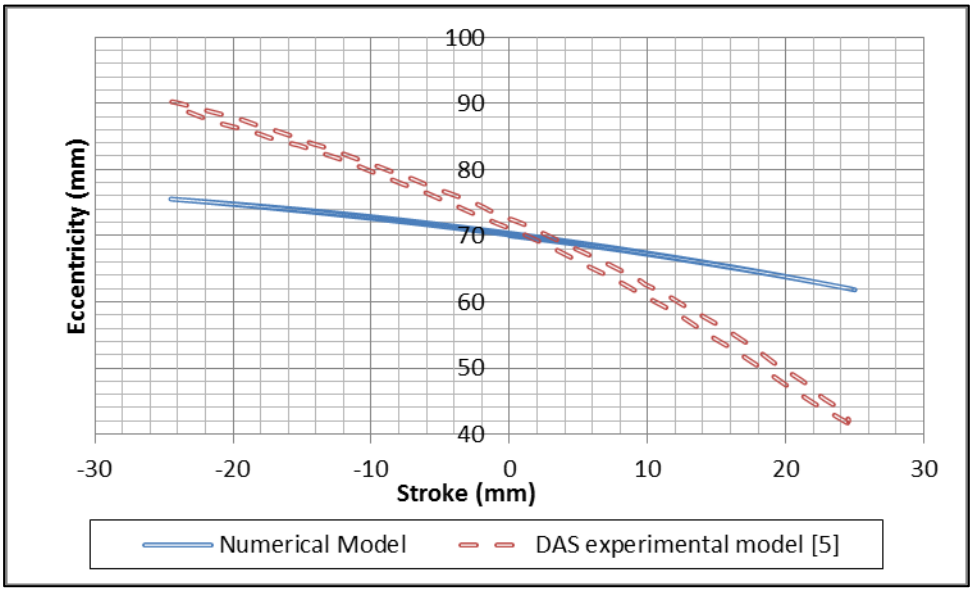

Figure 3-9: Load eccentricity and actuator stroke

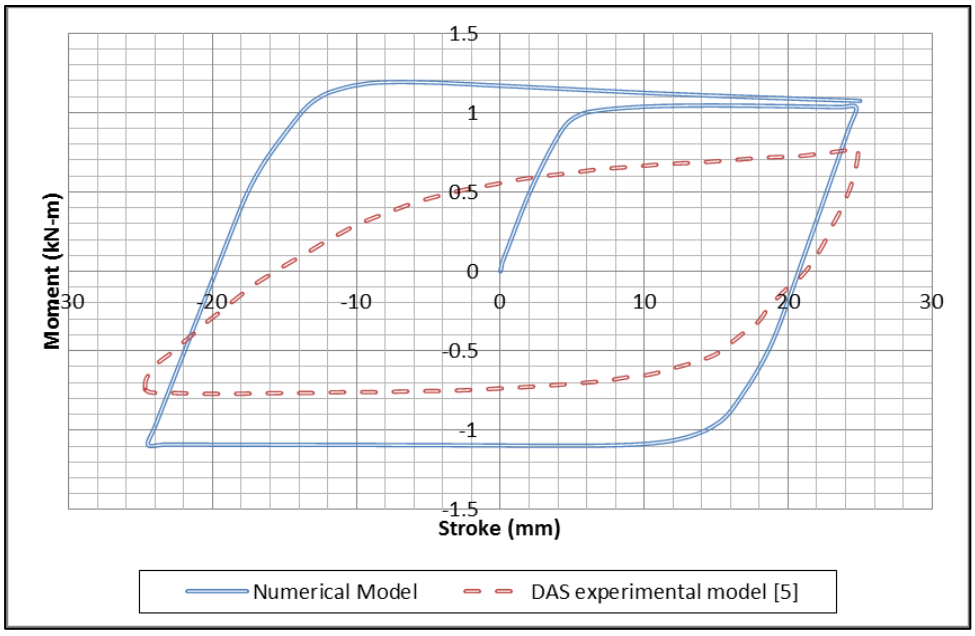

Figure 3-10: Moment vs. Stroke

A series of FE modelling procedures were developed to assess the significance of kinematic hardening through the monotonic loading, associated with the bending of the strip specimen, and cyclic loading of the V-shaped coupon.

Standard tensile coupon geometry was modelled (Fig. 3-11) and the coupon constitutive model was defined with nonlinear, kinematic hardening parameters to characterize translation of the yield surface and isotropic hardening component to characterize the size evolution of the yield surface. Yield was defined by the von Mises criterion with an associated flow rule implemented.

Parameters for the kinematic plasticity model were defined for two material types that included (1) conventional definition with the yield stress specified at 0.5% strain and (2) yield stress defined at the onset of nonlinear stress-strain behaviour. Also the parameters were selected to isolate the effects of kinematic translation and isotropic expansion of the yield surface on the stress-strain and hysteric moment response. The parameters are summarized in Table 3.3.

As shown in Fig. 3-12, the stress-strain behaviour of the simulated coupon tests, when using the kinematic hardening model, provided good correspondence with the baseline Ramberg-Osgood type relationship. On this basis, Bauschinger effects on the cyclic response could be evaluated.

	σ_y (MPa)	Kinematic Hardening Parameter	Y	Equivalent Stress (MPa)	Q_∞ (MPa)	Hardening Parameter b
1	358	100000	6000	358	358	3.5
2	188	200000	1200	188	188	13.2

Table 3-3: Parameters for kinematic hardening models

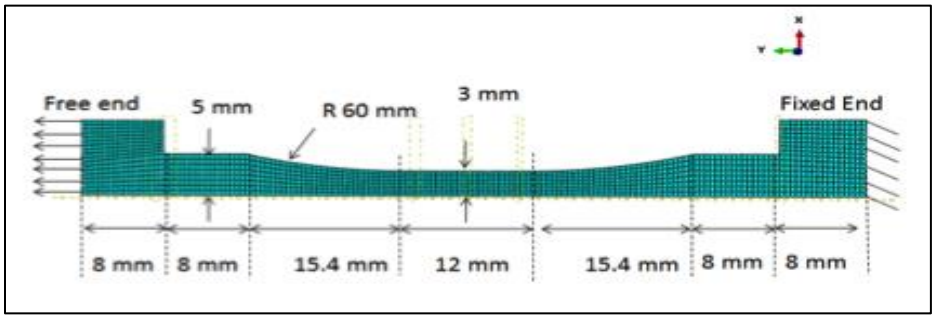

Figure 3-11: Tensile coupon dimensions and boundary conditions

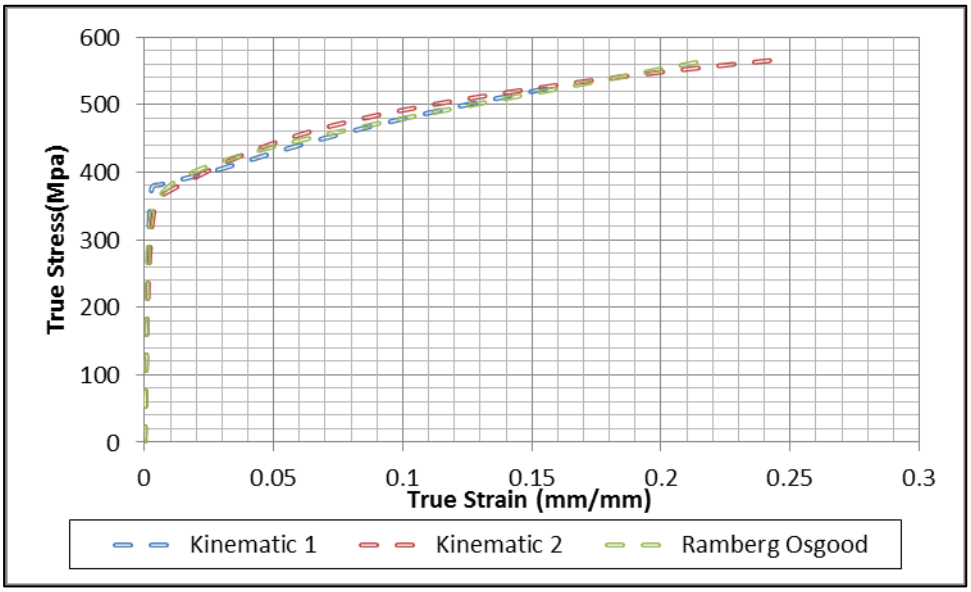

Figure 3-12 : True stress–strain relationships

As shown in Fig. 3.13, the cyclic load event on the V-shaped coupon bending strip does not exhibit Bauschinger effect for any material model examined. The isotropic model and kinematic model (1) characterize material behaviour with increasing strain (i.e. kinematic shift) and limited expansion of the yield surface (i.e. isotopic expansion). The kinematic model (2) characterizes material behaviour with limited kinematic shift and greater expansion response of the yield surface.

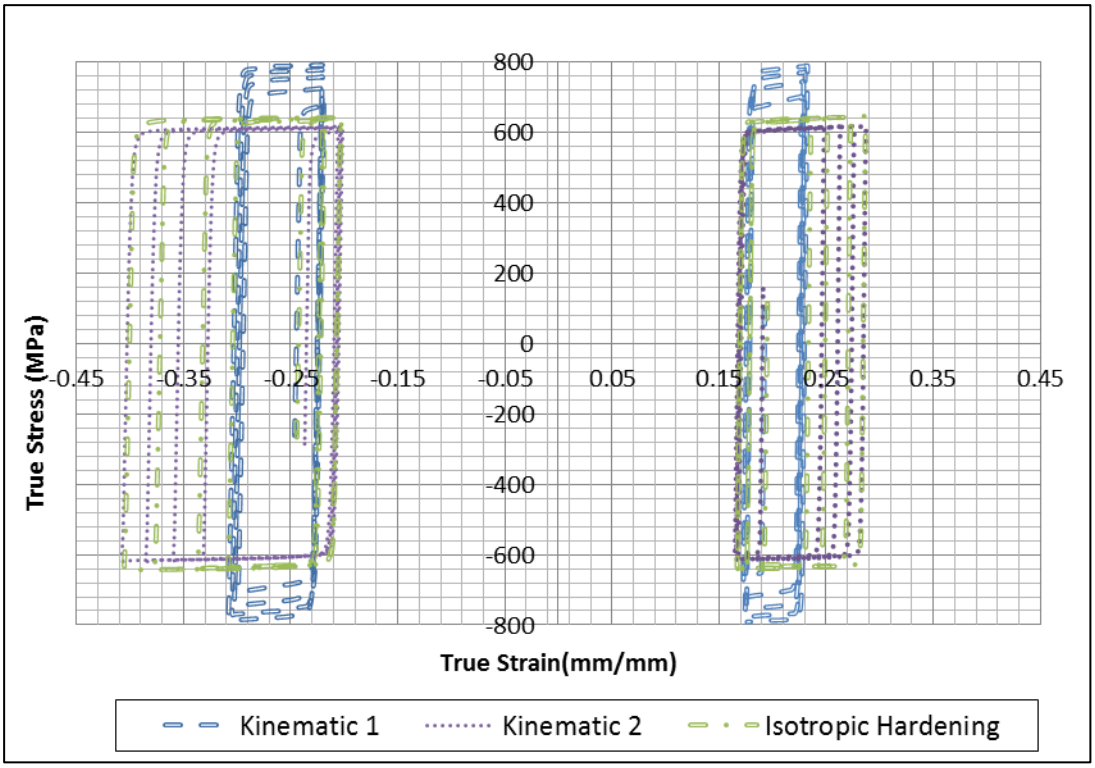

Figure 3-13: True stress–strain behaviour during cyclic load events for coupon with different constitutive models

Although the coupon stress-strain response exhibited different characteristics for each constitutive model, with the corresponding material parameters, the influence on the

predicted hysteric response was not significant (Fig. 3-14.). The limited sensitivity analysis suggests the discrepancy between the numerical simulations and the experimental test is probably related to the boundary conditions that may include the application of the actuator stroke, transformation of the actuator stroke from linear translation to rotation of the bend radius apex through the loading mount and relative stiffness effects associated with the coupon, loading mount and test frame. Future numerical studies will investigate this hypothesis.

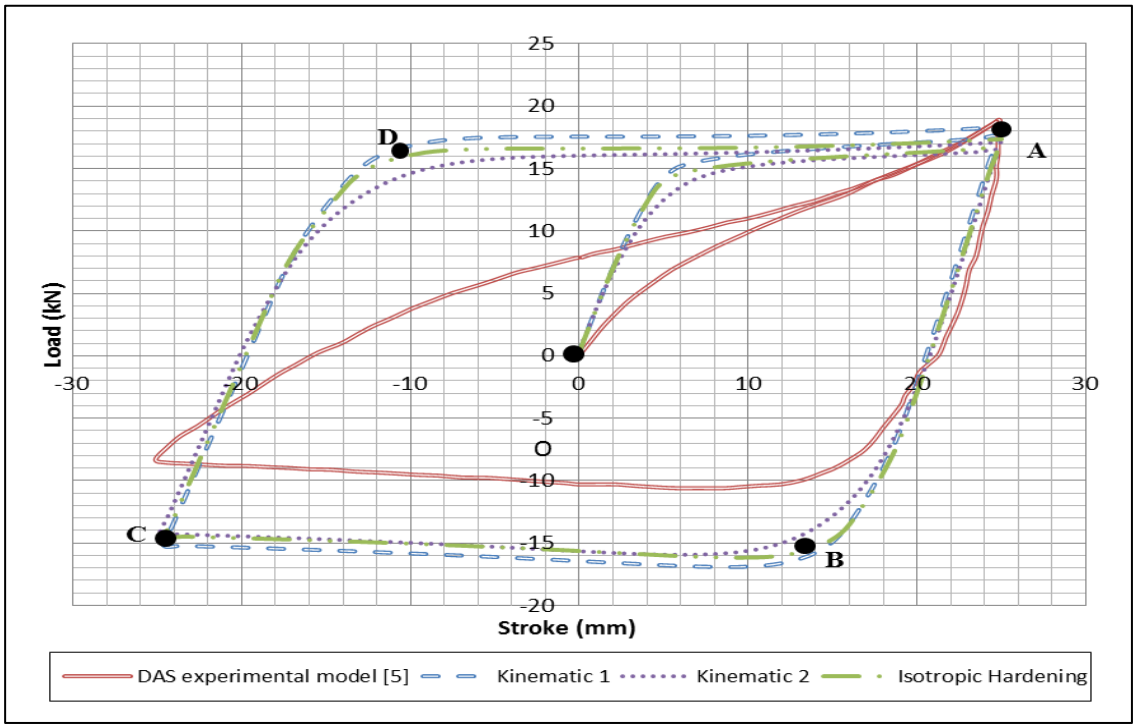

Figure 3-14: Hysteresis loop for coupon with different constitutive models

3.8 Conclusions

Numerical modelling procedures have been calibrated to simulate the bending of a straight pipe segment strip to a V-shaped coupon used to evaluate the low cycle fatigue

(LCF) life performance of wrinkled pipe segments. The analytical estimates and numerical predictions of residual strain for the V-shaped coupons were consistent. There was greater uncertainty in the hysteretic behaviour when comparing the response between the experimental measurements and numerical simulations. The primary reason for this discrepancy was the differences in kinematic boundary conditions imposed on the V-shaped coupon that influenced the load eccentricity (i.e. imposed moment across the coupon) for the opening and closing modes. For the parameters examined, the numerical sensitivity analysis suggested the hardening model did not significantly influence the load hysteretic response of the V-shaped coupon. Further experimental and numerical studies are required to address and substantiate the observed discrepancies and advance a calibrated simulation tool.

3.8 Acknowledgements

The authors would like to acknowledge the Wood Group Chair in Arctic and Harsh Environments Engineering at Memorial University of Newfoundland for sponsoring the research project. The opportunity to conduct the research and publish the findings of the project is greatly appreciated.

3.9 References

ABAQUS Extended Functionality HTML Documentation, Version 6.9

Bai, Y., Knauf, G., Hillenbrand, H.G. (2008). “Materials and design of high strength pipelines”, Proc., ISOPE,

Bouwkamp, G., Stephen, R.M. (1973). “Large Diameter Pipe under Combined Loading”, Transportation Engineering Journal of ASCE, 99(TE3): 521 – 536, 1973

Bruton, D., Carr, M., Crawford, M and Poiate, E. (2005). "The safe design of hot on-bottom pipelines with lateral buckling using the design guideline developed by the SAFEBUCK Joint Industry Project." Proc., DOT, 26p.

Das, S., Cheng, J.J.R., Murray, D.W. (2007). "Prediction of the fracture life of a wrinkled Steel pipe subject to low cycle fatigue load", Can. J. Civ. Eng., 34:598-607.

Das, S. (2003). "Fracture of wrinkled energy pipelines." Ph.D., University of Alberta, 152-180, 252p.

Das, S., Cheng, J.J.R., Murray, D. and Nazemi, N. (2008). "Effect of monotonic and cyclic bending deformations on NPS12 wrinkled steel pipeline." J. Strct. Eng. 134:1810-1817.

Das, S., Cheng, J.J.R., and Murray, D. (2008). "Prediction of fracture in wrinkled energy pipelines subjected to cyclic deformations." IJOPE 17(3):205-212

Halford, G.R. (1986) "Low-cycle thermal fatigue." NASA Technical Memorandum 87225, 120p.

Jayadevan, K.R., Ostby, E., Thaulow, C. (2004). "Strain based fracture mechanics analysis of pipelines", ICAS/04-0198, Proc., Int. Conf. Advances in Structural Integrity, Paper # ICAS/04-0198.

Junak, G. and Cieśla, M. (2011). "Low-cycle fatigue of P91 and P92 steels used in the power engineering industry." Archives of Mat. Sci & Engng, 48(1):19-24.

Mahdavi, H., Kenny, S., Phillips, R. and Popescu, R. (2010). "Effect of soil restraint on the buckling response of buried pipelines." Proc., IPC2010-31617, 10p.

Michailides, D. and Deis, T. (1998). "Internal measurement and mechanical caliper technology." Proc., IPC, 373-378p.

Myrholm, B.W. (2001) "Local buckling and fracture behaviour of line pipe under cyclic loading." M.Sc., University of Alberta,43-59, 190p.

Scotberg, T. and Bruschi, R. (1992). "Future pipeline design philosophy – Framework." In Proc., of the International Conference on Offshore Mechanics and Arctic Engineering, Calgary, Alta., 7-12 June 1992.Offshore Mechanics and Arctic Engineering (OMAE) Division of the American Society of Civil Engineers (ASME), Washington, D.C Vol 5(A) 239-248p

Sugiura, K., Chang, K.C., Lee, G.C. (1989) "Evaluation of Low Cycle Fatigue Strength of Structural Metals", Journal of Engineering Mechanics, ASCE, 117(10): 2373-2383

Xue, L. (2008). "A unified expression for low cycle fatigue and extremely low cycle fatigue and its implication for monotonic loading." Int. J. Fatigue 30:1691-1698.

Yao, J.T.P. and Munse, W.H. (1961). "Low-cycle fatigue of metals – Literature review." Ship Structure Committee, U.S. Department of the Navy, Serial No. SSC-137, 37p.

Zhang, J. (2010). "Development of LCF life prediction model for wrinkled steel pipes" Ph.D., University of Alberta, 18-27, 56,151-154,320p.

3.10 Annex A – Variation of Residual Strain

Test Specimen		FEA Analysis		Theoretical Analysis (1)	Physical Test (2)	Physical Test (3)		Difference(4)	
	R/t	Outside Surface	Inside Surface	Outside / Inside Surface	Outside Surface	Outside Surface	Inside Surface	Outside Surface	Inside Surface
X52-T6-A45-R20-S50	3.33	0.152	-0.149	+/- 0.123	0.19	-	-	18.90%	-
X52-T9-A45-R20-S50	2.41	0.216	-0.210	+/- 0.159	0.21	-	-	3.02%	-
X52-T12-A45-R20-S50	1.68	0.299	-0.316	+/- 0.206	-	-	-	-	-
X65-T6-A45-R20-S50	3.33	0.153	-0.150	+/- 0.123	-	0.136	-0.138	12.39%	8.45%
X65-T9-A45-R20-S50	2.41	0.214	-0.215	+/- 0.159	-	0.186	-0.173	15.44%	24.03%
X65-T12-A45-R20-S50	1.68	0.303	-0.314	+/- 0.206	-	0.255	-0.252	18.86%	24.45%

Table 3-4: Variation of Residual Strain

(1) Theoretical Strain was obtained by Equation (1) and was converted into True Strain

(2) Results for physical tests were obtained from Das (2003)

(3) Results for physical tests were obtained from Zhang (2010)

(4) Difference is calculated between results from physical tests and FEA results

4 DEVELOPMENT OF A FATIGUE LIFE ASSESMENT TOOL FOR PIPELINES WITH LOCAL WRINKLING THROUGH PHYSICAL TESTING AND NUMERICAL MODELLING

This peer reviewed paper has been published in the proceedings of International Conference on Ocean, Offshore and Arctic Engineering (OMAE 2014-24082, San Francisco, U.S.A.). This paper was a collaborative effort that included myself, technicians at Memorial University and Dr. Shawn Kenny. As the primary author, I was responsible for conducting the physical tests, analysing the data, developing the numerical algorithms and simulation tools, and synthesizing the results within this paper. David Snook and William Bidgood were responsible for fabrication of the strip sample whereas Mathew Curtis was responsible for the instrumentation setup during the testing. Dr. Shawn Kenny was responsible for providing supervision and guidance during this study and editorial comments in the preparation of this paper.

Authors: Fahad Bakhtyar and Shawn Kenny

4.1 Abstract

Pipelines are one of the primary modes to transport hydrocarbon products throughout the world. A majority of these pipeline systems are buried, which are susceptible to ground movement that imposes axial forces and bending moments on the pipeline section. As a result of these forces and moments pipeline section may experience localized deformation that result in wrinkling, buckling and other damage mechanisms. This may impair the

pipeline mechanical performance with respect to local stress concentration, lower strength and reduced fatigue life. Cyclic operational loads or ground movement events may result in strain reversals within the pipeline section that may lead to fracture through low cycle fatigue process.

In this study, physical testing was conducted to examine the strength and fatigue life performance characteristics of hot rolled steel (44-W). The effects of the test sample bend radius, wall thickness and imposed displacement stroke range on fatigue performance were examined. The data was used to develop and refine continuum finite element modelling procedures that can be used to assess the influence of pipeline damage on fatigue life in a more detailed numerical simulation framework.

4.2 Introduction

Pipelines are an efficient mode of transport for crude oil and other refined products from the resource base to end users. According to the Canadian Energy Pipeline Association (Canadian Energy Pipeline Association) pipeline contribute $8.8 billion to the Canadian Gross Domestic Product (GDP) with more than $84 billion worth of Canadian oil, gas and petroleum products for export in 2012. The buried natural gas and liquids pipeline network is estimated to be 830,000 km in Canada with billions of dollar projects under way to add to this network.

These buried pipeline systems may be located in onshore and offshore regions with large magnitude, relative ground displacement events including subsidence, long term slope

movement, seismic faulting and ice gouging (Kenny et.al (2007)). In northern regions with ground permafrost, thaw settlement and frost heave mechanisms may also impose large relative ground displacement on the buried pipeline. In response to operational loads (i.e. pressure and temperature) and relative ground movement, load transfer mechanisms through pipeline/soil interaction events impose axial loads and bending moments on the buried pipeline. The pipeline may experience localization of these forces through deformations mechanisms such as ovalization and local buckling (Kenny et. al(2007),Gresnigt (1986), Mahdavi et.al (2010), Doblanko (2002)). Although the pipe section becomes distorted with large strain gradients experienced across the local buckle crest, for monotonic loading conditions, physical modeling and numerical simulations studies have demonstrated the integrity of the pipeline system may not be compromised (Gresnigt et. al (2001), Al-Showaiter et. al (2011), Fatemi et. al (2012), Jayadevan et. al (2004), Suzuki et. al(2007)).

However, recent investigations have shown the potential for pipeline fracture and loss of pressure containment (i.e. through wall rupture) through low cycle fatigue mechanism (Myrholm (2001), Das et.al, Das (2003), Bakhtyar et.al (2013), Zhang (2010)). Due to the initial damage state, the effects of cyclic loading, which may result from transient conditions during operation (e.g. shut-in and re-start) and repeated ground movement events, are amplified that may result in a loss of mechanical integrity. In these investigations, a fracture life assessment model was proposed based on physical coupon tests and finite element models simulating the local buckle geometry subjected to cyclic

load events. These studies examined a range of stroke displacement, bend radius and wall thickness. The bend radius was used to characterize the shape of the local wrinkle.

There remains some uncertainty on the governing parameters influencing low-cycle fatigue that hinders the development of engineering tools for predicting the remaining fatigue life of pipelines with local damage; such as local wrinkling. Increased knowledge will allow for strategic implementation of operational, maintenance and intervention programs to extend pipeline life and repair when needed, which would save millions of dollars related to unnecessary intervention or reactive remediation (Søtberg et.al (1992), Michailides et. al (1998)).

This study is a continuation of a previous investigation on the low-cycle fatigue response of pipeline with local damage (Wang et. al (2002). A series of experiments on mechanical test coupons, representing local damage in a pipeline segment, was conducted on hot-rolled steel based on locally available materials. Although physical data exists in the public domain (e.g. Myrholm (2001), Das (2003)) some key parameters have not been reported that hinder the verification of numerical simulation tools and assessment of numerical model uncertainty. The experimental data was used to calibrate continuum finite element modelling procedures. The numerical model was used to conduct a limited evaluation on low cycle fatigue using the experimental data from this study and extended to pipeline steels using available data in the public domain.

These investigations are described in further detail with the key results presented in this paper. A discussion on the outcomes is presented with a focus on the development of an

engineering tool to predict the low-cycle fatigue life of a pipeline with an initial damage state. The requirements to refine and verify the continuum finite element modelling procedures is also presented. An improved and verified numerical simulation tool can then be used to conduct a more comprehensive parameter study addressing low cycle fatigue of damaged pipelines across a range of practical design parameters.

4.3 Experimental Testing

4.3.1 Overview

In this study, the effect of local damage on the low cycle fatigue response of hot rolled steel (44W) was investigated through physical tests using a "strip coupon". Due to the lack of available pipe steel grade material, hot rolled steel samples were used. A V-shaped strip coupon, illustrated in Fig. 4-1, was fabricated from stock metal through cold cutting and cold working procedures.

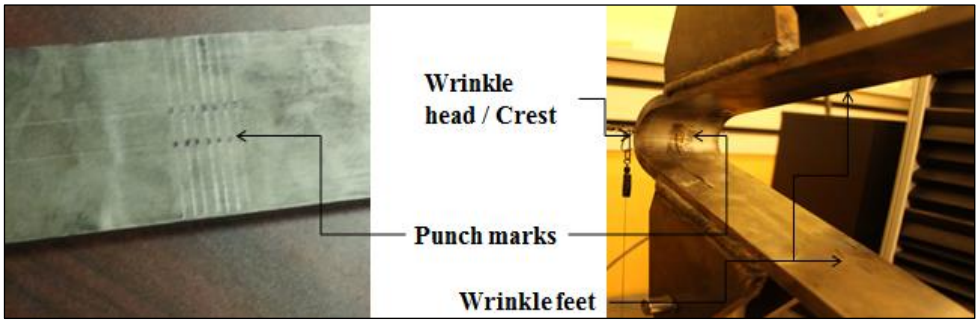

Figure 4-1: Strip Coupon

A cold cut method was used, for mitigating the development of residual stresses, to fabricate the samples, with dimensions of 535 mm in length and 63.7 mm in width. In

University of Alberta (UoA) investigations, a strip width of 57 mm was used (Das et. al , Das (2003)). In comparison with this study, there was no observed discrepancy in the mechanical performance or residual low cycle fatigue life response due to the greater strip specimen width being used. Mechanical properties for the hot rolled steel (44W) are summarized in Table 4-1. The characteristic stress-strain relationship is illustrated in Fig. 4-2.

Strain Rate	0.0067	mm/mm/s
Yield Strength	366	MPa
Elastic Modulus	220	GPa
UTS	541	MPa
Fracture Strength	411	MPa
Fracture Strain	0.362	mm/mm
% Elongation	36.2	%
% Reduction Area	49.7	%

Table 4-1 Material properties for Hot Rolled Steel

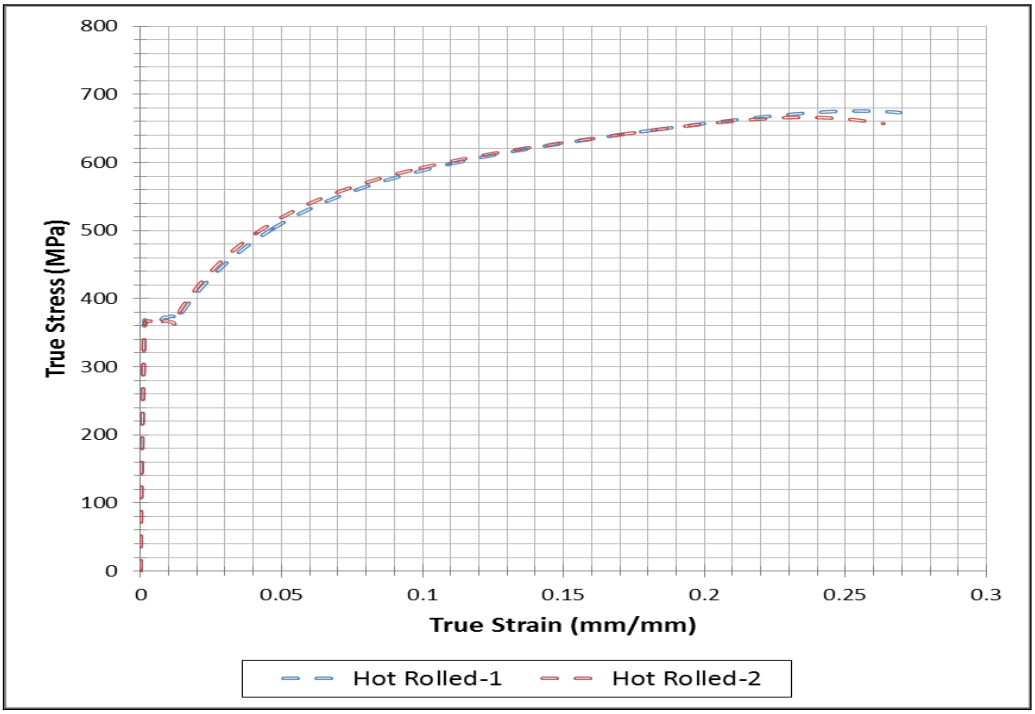

Figure 4-2: Characteristic True Stress-Strain Relationship

Three different wall thicknesses were investigated including 6.35 mm, 9.7 mm and 12.7 mm. The strip coupon was bent at mid length in the longitudinal direction at an angle of approximately 45^0 with bend radii of 10 mm, 15 mm or 20 mm. The cold work procedure was similar to the approach of other studies (Das et. al, Das (2003)) and, in a previous investigation, simulated through numerical modeling procedures (Bakhtyar et. al (2013)). This provided a range of bend radius to wall thickness ratios (R/t), of 0.8 to 3.2, for the experimental investigations.

As shown in Fig. 4-1, the strip specimen can be characterized by two main features including the wrinkle crest (head) and strip test coupon support (foot). The wrinkle crest is the zone of local damage representing the effects of local buckling on a deformed

pipeline segment (Myrholm (2001), Das (2003), Bakhtyar et. al (2013), Zhang (2010)). The strip coupon support is the location of the applied actuator stroke that imparts a compressive and tensile bending moment on the wrinkle crest.

During the forming process to fabricate the V-shape strip coupon, which was a monotonic cold work bending process, a series of punch marks were used to measure residual strain patterns. The punch marks were set along two parallel rows, on both the inside (intrados of the bent strip) and outside (extrados of the bent strip) surfaces, along the longitudinal axis of the strip test coupon near the wrinkle crest location (Fig. 4-1). The distance between the two rows was 10 mm and between any two adjacent punch marks was 5 mm (Fig. 4-1). The distance between punch marks, before and after the cold work bending process, was measured using an electronic Vernier caliper. The residual bending strain, which is a measure of the remaining strain after deforming the strip coupon less any elastic rebound, was compared with the analytical solution expressed by

$$\epsilon = \frac{1}{\left(1 + \frac{2R}{t}\right)} \qquad \text{Eq. 4.1}$$

where, R is the radius of the wrinkle and t is the thickness of the coupon.

The strain due to bending (Eq. 4.1) is based on the idealizations formulated in beam theory that include plane sections remain plane with no distortion over the cross section. As shown in Fig. 4-3, the measured residual strain compares well with the analytical expression (Eq. 4.1) across the range of R/t ratios examined.

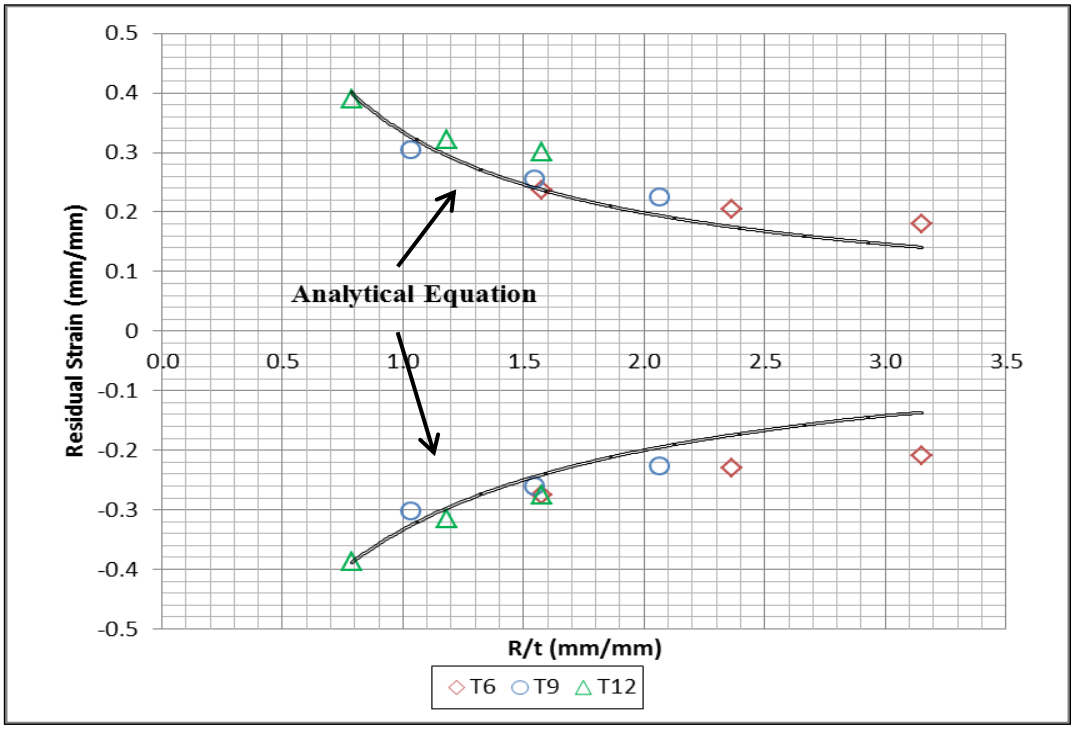

Figure 4-3: Residual Strain as a Function of R/t for a Range of Wall Thickness Strip Coupons

To identify each strip sample, a designation system was used T6-R15-A45-S50 with T indicating nominal wall thickness, R for bend radius, A for bend angle and S for the actuator stoke. A total of 27 strip specimens were tested for the remaining low cycle fatigue life experiments with the test matrix and data summarized in Annex A.

Eccentricity is defined as the shortest distance between the wrinkle crest and load line (i.e. actuator stroke path). The initial eccentricity (e_o) was set at 70 mm, which is consistent with previous studies (Das (2003), Bakhtyar et. al (2013), Zhang (2010)). During the cyclic load event, the eccentricity decreased in the opening mode (i.e. positive

tension load) and increased in the closing mode (i.e. compressive load). The eccentricity can be expressed as

$$e = e_o + \delta_e \qquad \text{Eq. 4.2}$$

where the change in eccentricity (δe) was measured using a series of string potentiometers.

In order to impose the displacement stroke for the cyclic loading events, two griping plates were welded onto each strip specimen. The dimensions of the gripping plates were 103 mm in length and 12 mm in width (Fig. 4-4). The loading plates were aligned on the strip specimen to produce an initial eccentricity of 70 mm with respect to the vertical loading axis of the Instron 5585H test machine. The gripping plates were attached to the actuator and load plates of the Instron test machine through transition load mounts that imposed only vertical bearing forces.

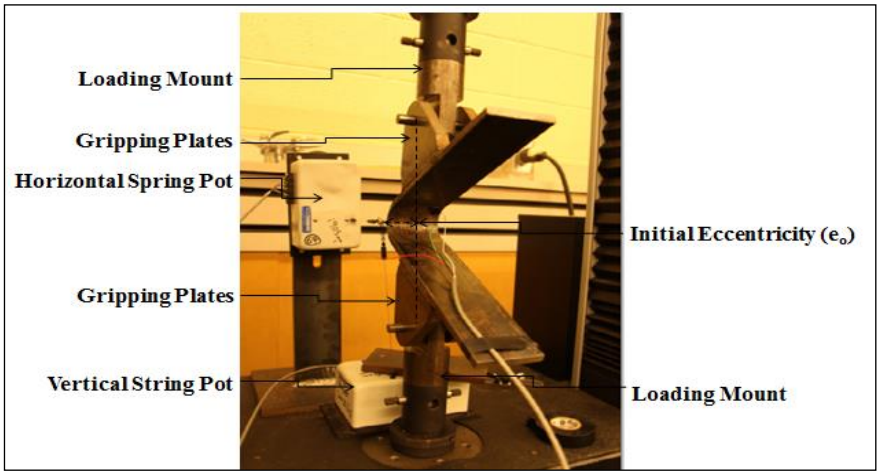

Figure 4-4: Initial Setup within Test Frame

Electronic strain gauges were also attached to the wrinkle crest of the strip coupon but debonded from the strip coupon surface with subsequent load cycles. In low cycle fatigue, loading rate plays an important role as too fast would lead to heat loss and too slow will yield creep into the sample (Wang et.al (2002)). The loading rates were set identical to those used in previous research studies as 11.45 mm/min, 10.64 mm/min and 8.05 mm/min for an applied actuator stroke of 20 mm, 50 mm and 80 mm; respectively (Zhang (2010)).

4.3.2 Results and Discussions

A typical load-stroke hysteresis loop, from the physical testing program, for the first compression-tension load cycle is illustrated in Fig. 4-5 for two samples T9-R10-A45-S20 and T9-R10-A45-S50. The initial load segment OA represents the strip coupon response to the applied tensile load from the initial configuration, with 70 mm eccentricity, due to opening of the wrinkle crest bend angle. The segment ABCD

represents the compressive stroke cycle (i.e. closing mode) with decreasing wrinkle crest bend angle. The line segment DEFG represents the subsequent tensile load response with a return to the open configuration. This cyclic loading-unloading loop (ACDA) was repeated until the strip coupon fractured at the extrados crest.

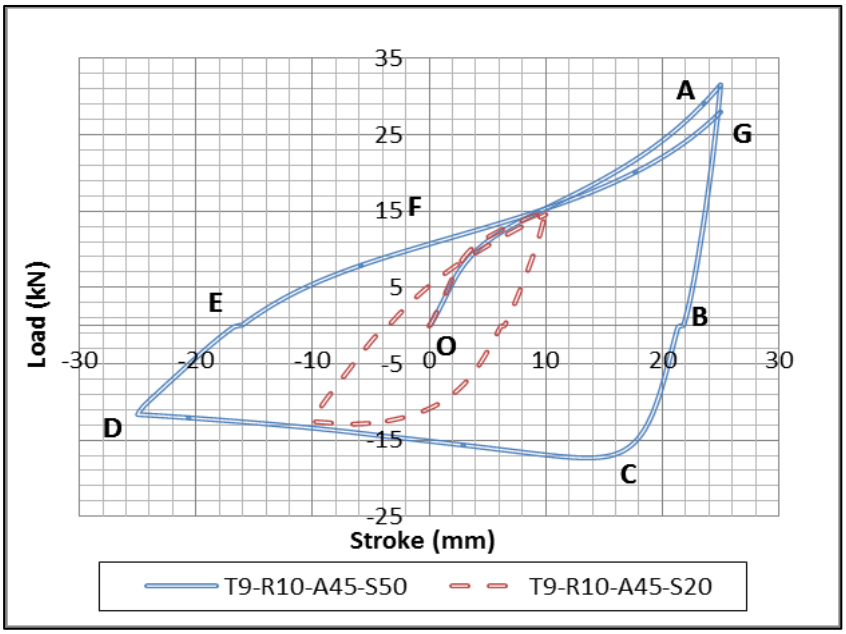

Figure 4-5: Load-Stroke Hysteretic Loop

The stroke amplitude was a significant influence on the hysteretic loop response with respect to the characteristic shape and evolution of plastic deformation. For increasing stroke displacement, from 20 mm to 80 mm, the characteristic shape of the load-stroke hysteretic loop was observed to have greater asymmetry through the load cycle. In a single load cycle, for strip coupons with 20 mm stroke amplitude, the unloading curve segment was twice as stiff as loading curve segment; whereas for 50 mm and 80 mm stroke range the relative stiffness was different by a factor of 6 and 15, respectively.

As shown in Fig. 4-5 for the 50 mm stroke amplitude load case, the maximum tensile load was obtained at the maximum positive stroke (Point A or G) or maximum (opening) angle; whereas the maximum compressive load was obtained at point C rather than at the maximum compressive stroke amplitude or minimum (closing) angle (Point D). For stroke amplitude of 20 mm the ratio between the maximum tensile load and maximum compressive load was 1.2; whereas, for a stroke of 50 mm the ratio was 1.8.

These observations on the response characteristics of the hysteretic loop (Fig.4-5) indicate a relationship between the nonlinear stiffness and mechanical work hardening response of the strip coupon with respect to the specimen geometry and orientation in relation with the imposed stroke displacement and amplitude. The influence of stroke amplitude on the low cycle fatigue response is further addressed in later in this section.

The load eccentricity also exhibited a nonlinear response with the applied displacement stroke magnitude (Fig. 4-6). Tension loading (i.e. positive stroke) tends to open the wrinkle crest angle and reduce the eccentricity, where the actuator stroke is restrained along a fixed line in the Instron test frame (Fig. 4-4). Compression loading (i.e. negative stroke) tends to close the wrinkle crest bend angle and increase eccentricity. For a stroke of 20 mm, the relative change in the eccentricity with the initial starting point (i.e. 70 mm) was an identical $\pm$10 mm change in eccentricity amplitude. For a stroke of 50 mm, however, the eccentricity increased by 22 mm through the compression stroke but decreased by 32 mm on the tension cycle. The eccentricity was used to estimate the applied bending moment at the strip coupon wrinkle crest during the cyclic loading event.

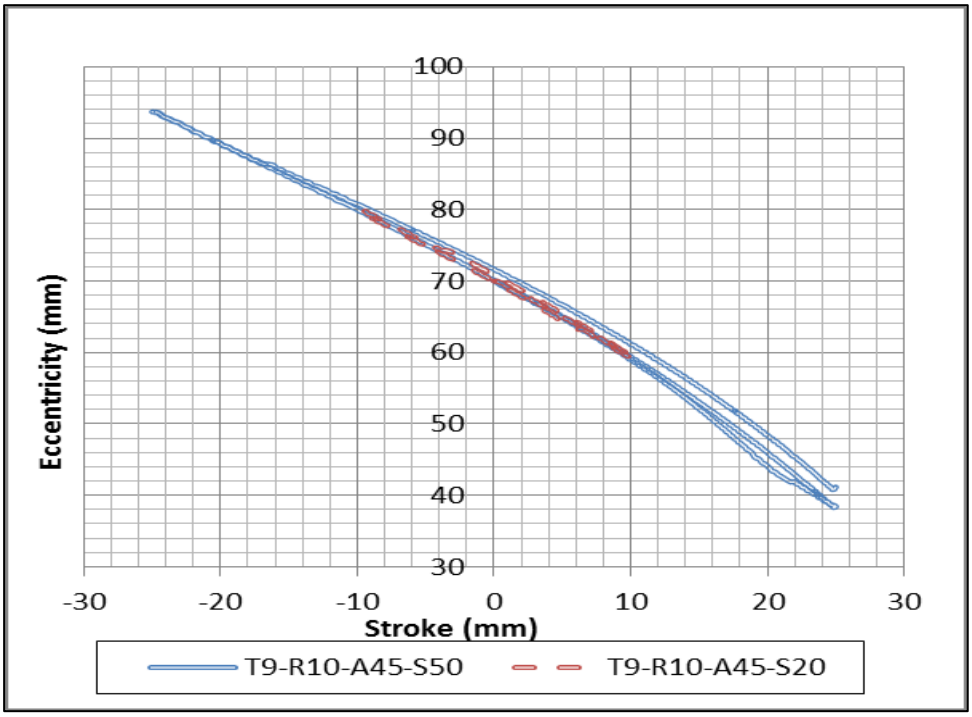

Figure 4-6: Nonlinear Eccentricity-Stroke Relationship

In comparison with the load-stroke hysteretic loop (Fig. 4-5), the wrinkle crest moment-stroke hysteretic loop exhibited a more symmetric response, particularly at lower stroke displacement amplitudes (Fig. 4-7). The maximum opening (tensile) and closing (compressive) moments were effectively the same magnitude. In contrast with the load-stroke hysteresis loop response (Fig. 4-5), the maximum compressive moment occurred at the maximum compressive stroke. Similar to the differences observed in the loading and unloading stiffness of the load-stroke hysteretic loop (Fig. 4-5), the slope of the unloading curves was 1.4, 2.6 and 3.2 times greater than the loading curve for stroke 20 mm, 50 mm and 80 mm; respectively.

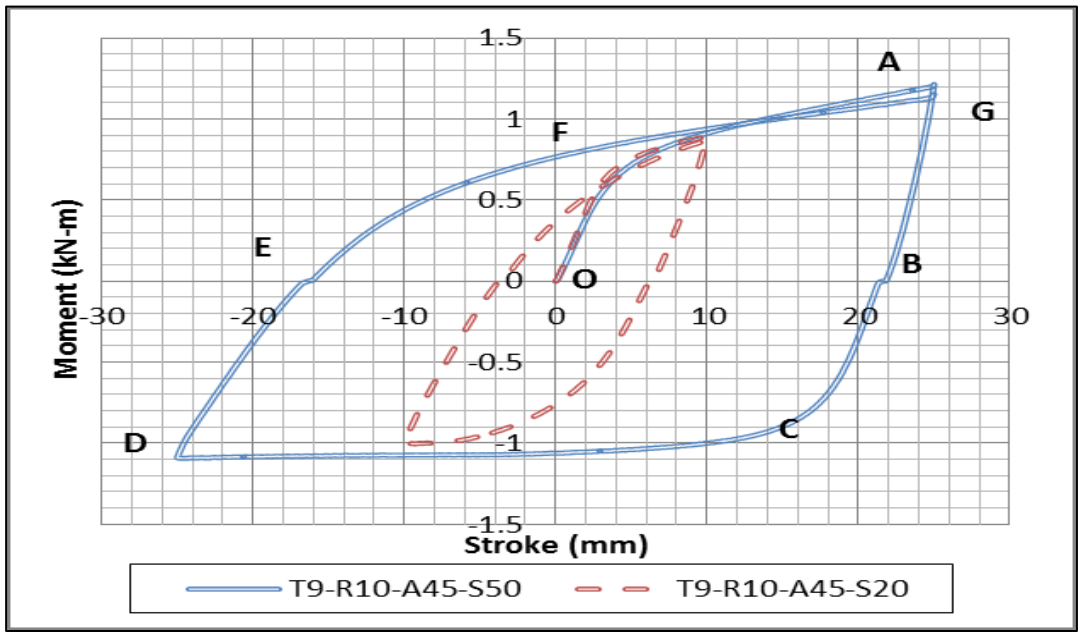

Figure 4-7: Moment-Stroke Hysteretic Loop

Previous research defined the term Hysteresis Loop Energy (HLE), which refers to energy absorbed by the crest during the cyclic loading and unloading or in other words it is the measure of the damage per unit cycle, which was denoted by U_o (Myrholm (2001), Das (2003)). In this study, the strain energy density (U_o/V) was examined, which is a scalar quantity on the relationship between stress and strain per unit volume. The bend strip wall thickness, width and arc length between the test supports at the gripping plates (Fig. 4-4) defined the strip coupon volume.

Based on the strip coupon experiments conducted in this study, a power law relationship was observed between the strain energy density (U_o/V) and the number of cycles to failure (N_s) as shown in Fig. 4-8. As the R/t ratio increased, for defined stroke amplitude, the strain energy density, for the first load cycle, decreased and the number of cycles to

failure increased. This relationship is related to the initial damage state (i.e. residual strain), and strain energy absorbed due to the strain demand (i.e. stroke displacement and bending moment) imposed on the strip coupon and plastic strain response at the wrinkle crest.

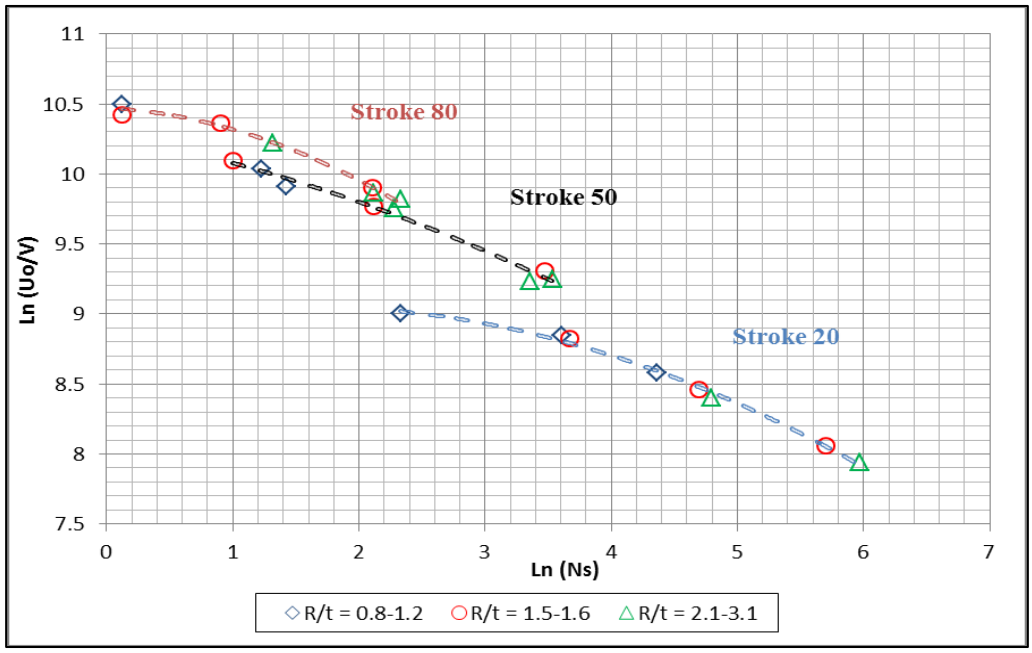

Figure 4-8: Number of Cycles to Failure (N_s) as a Function of the Strain Energy Density (U_o/V) for Varying R/t

For increasing R/t, the residual strain (i.e. initial damage state), as shown in Fig. 4-3, and strain energy density (Fig. 4-9), for the first load cycle, was observed to decrease. Thus for a specific stroke amplitude the number of load cycles to failure increases with R/t for specific stroke amplitude (Fig. 4-8). The incremental damage or strain energy absorbed during the first load cycle was observed to increase with increasing stroke amplitude and wall thickness (Fig. 4-10).

For nominally equivalent parameters, the results presented in Fig. 4-8, with respect to the influence of R/t, and Fig. 4-10, with respect to the influence of wall thickness, are consistent with other studies (Myrholm (2001), Das (2003), Zhang (2010)). Increasing the stroke range corresponds with greater strain energy density within a loading cycle. Increasing the wall thickness results in greater residual strain, for the same bend radius, and greater plastic strain energy for imposed displacement controlled loading conditions.

The experimental dataset in this study; however, suggests the imposed stroke displacement also influences the low cycle fatigue life. Based on the results (Fig. 4-8 through Fig. 4-10), there appears to be an upper shelf on the maximum strain energy density absorbed (or critical plastic strain increment per cycle) that influences the low cycle fatigue response. There appears to be a different relationship between strain energy density and number of cycles to failure when the imposed stroke amplitude is 20 mm in comparison with the 50 mm and 80 mm stroke amplitude dataset.

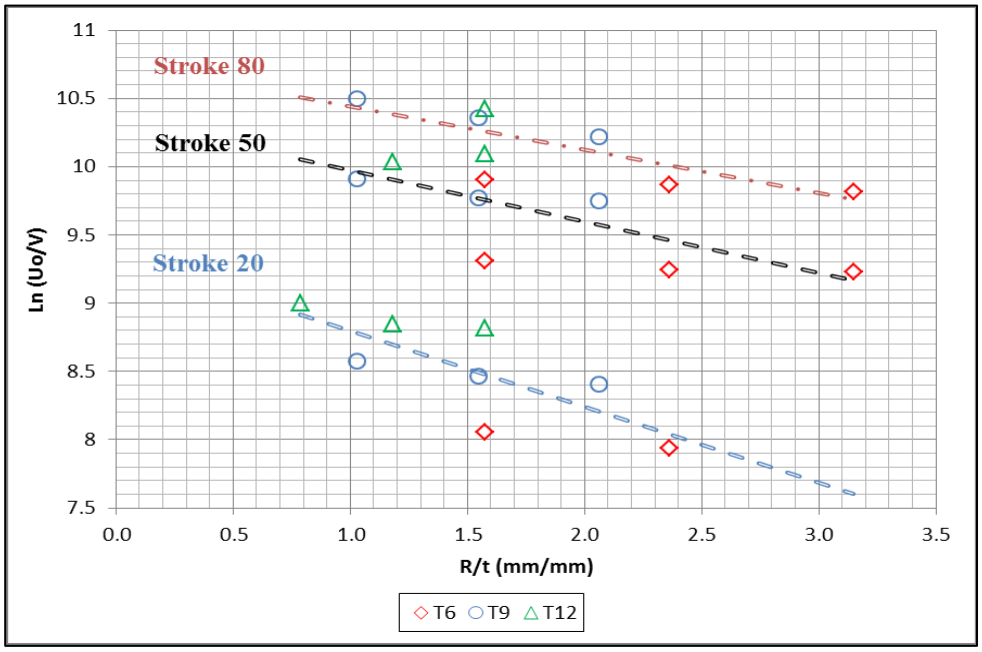

Figure 4-9: Strain Energy Density (U_o/V) Relationship with R/t, Wall Thickness and Stroke Amplitude

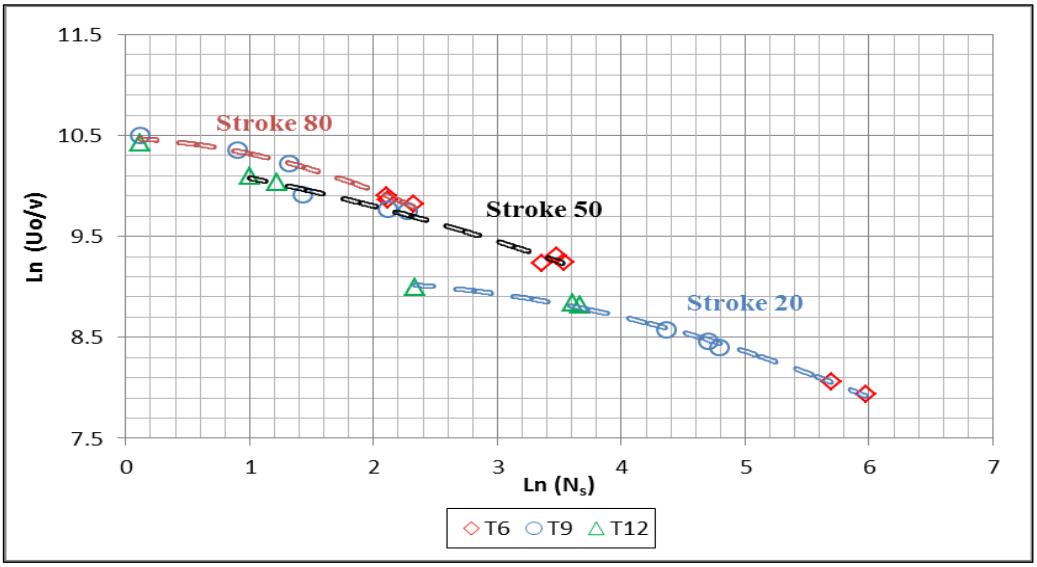

Figure 4-10: Number of Cycles to Failure (N_s) as a Function of the Strain Energy Density (U_o/V) for Varying Wall Thickness

As the imposed loading is displacement (i.e. stroke amplitude) controlled then it is expected the plastic strain gradient through thickness and along the wrinkle crest arc length should also vary in relationship with R/t, wall thickness and stroke amplitude. This is supported by the data illustrated in Fig. 4-10 where the strain energy density, for the first load cycle, increases with wall thickness for defined stroke amplitude.

The data (Fig. 4-8) was extrapolated to low values of strain energy density per load cycle as shown Fig. 4-11. The fatigue life performance, with decreasing strain energy density, was on the order of 106 cycles. This is consistent with fatigue strength estimates based on industry recommended practices (e.g. CSA Z662 (2010), DIN 2413 (1993) and DNV RP C203 (2010)).

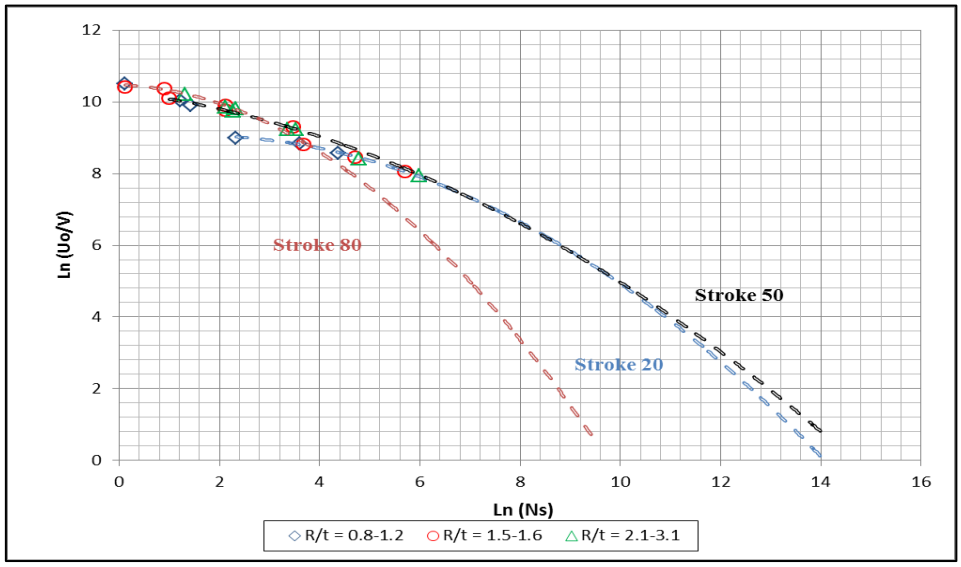

Figure 4-11: Extrapolation of Number of Cycles to Failure for Low Strain Energy Density Values

The initial damage state, strain demand per load cycle and mechanical behaviour has a significant influence on the low cycle fatigue response. As illustrated in Fig. 4-11, a characteristic function (e.g. linear damage rules) may describe the general relationship between strain energy density per cycle, or other parameter (e.g. wrinkle crest strain increment), and the number of cycles to failure. Early research expressed the low cycle fatigue response in terms of a power law relationship with the plastic strain amplitude, strain range or strain energy density (Coffin (1954, 1984), Morrow (1965), Manson (1954, 1966)).

The characteristic response illustrated in Fig. 4-11 is consistent with these past studies where strain energy may be used as a key parameter to estimate fatigue life performance for pipelines with local damage (Das (2003), Zhang (2010)). Furthermore, Zhang (2010)

provides a comprehensive framework where the low cycle fatigue prediction model was developed based on the strip coupon tests, large scale pipe tests and continuum finite element analysis. However, it is believed further investigations are required to address some areas of uncertainty before functional relationships with defined coefficients can be established with confidence.

There are a number of reasons for this statement. The correspondence between the strip coupon test analogue and the actual mechanical response of buried pipelines in the field requires further investigation. The relationship between bend radius, stroke amplitude, initial damage state and local plastic behaviour (Fig. 4-8 through Fig. 4-10) requires further investigation. The strip coupon may not best represent the initial damage state of a buried pipeline with a local wrinkle. The mechanical response and development of a local buckle is dependent on D/t ratio, internal pressure, global response, which may be influenced by the surrounding soil loads and restraint, and local effects; such as the presence of a girth weld (Mahdavi et. al (2010,2012), Al-Showaiter et. al (2011), Fatemi et.al (2012)). This may influence the initial damage state and deformation mechanisms with subsequent loading cycles, which may be a combination of axial, bending and torsional loads.

Furthermore, characterization of the damage initiation, accumulation and growth (e.g. crack length, growth mechanisms, and propagation rates) requires further experimental work, as supported by Zhang (2010). Due to the nature of the loading event, where the imposed geotechnical loads are primarily governed by displacement control process

where the use of stress based criteria for fatigue limits are problematic (Ellyin (1997)). Recent studies have highlighted the importance of multiaxial stress state, stress path, boundary conditions, material properties, geometry and constraint effects on the apparent toughness, fracture resistance and tensile strain capacity of pipelines (Kibey et. al (2009,2010), Cravero (2009)).

4.4 Numerical Modelling Procedures

4.4.1 Overview

Continuum finite element modelling procedures were developed to simulate the experimental testing program investigating the low cycle fatigue response of a strip coupon. Same modelling procedures as described in chapter 3 (Bakhtyar et.al (2013)). The objective was to calibrate the numerical modelling procedures using the experimental data, and conduct an expanded parameter study for the development of an engineering tool to predict the low cycle fatigue response of a pipeline with local damage. Although physical modelling studies have been conducted by e.g. Myrholm (2001), Das (2003), Zhang (2010) but it is difficult to establish the level of model uncertainty where some of the data required in the calibration study is limited, uncertain or not reported.

In this paper, a limited calibration study is presented. The results from the current experimental program and the work of Das (2003) are used to calibrate continuum finite element modelling procedures. The material property data is summarized in Table 4-1 and Table 4-2.

Thickness (mm)	6	8.3
Modulus of elasticity (GPa)	202	211
Proportional Limit (MPa)	314	378
Static yield Stress (MPa)	460	479
Static Ultimate Stress (MPa)	563	546

Table 4-2: Material properties as in literature Das (2003)

The strip coupon test TR-R10-A45-S50 from the current study and the strip coupon test X52-T9-A45-R20-S50 from Das (2003) were used in the calibration study.

4.4.2 Results and Discussions

A comparison between the numerical simulation and strip coupon test, based on data from this study, for the load-stroke relationship and moment-stroke relationship for the first load cycle is presented in Fig. 4-12.

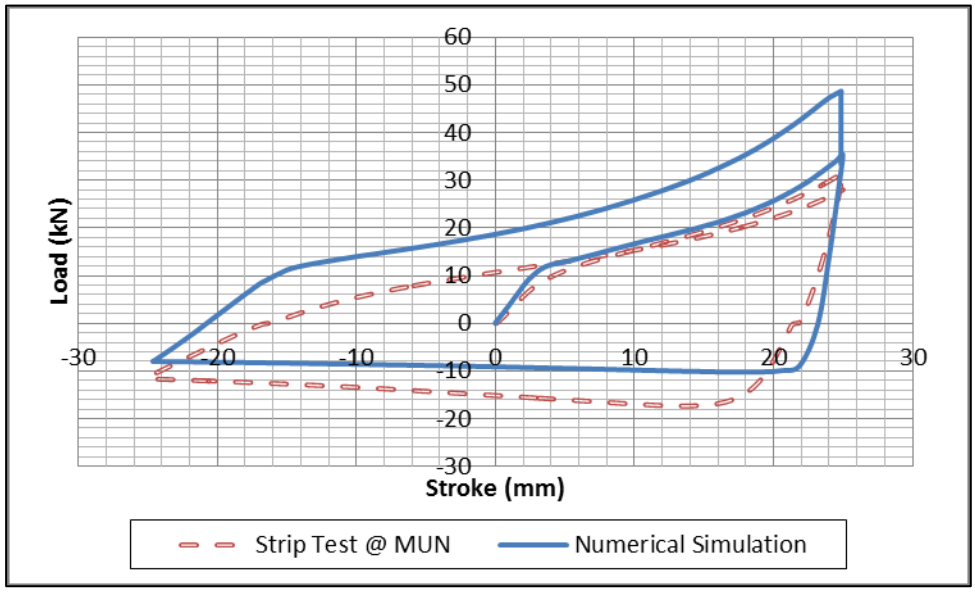

(a)

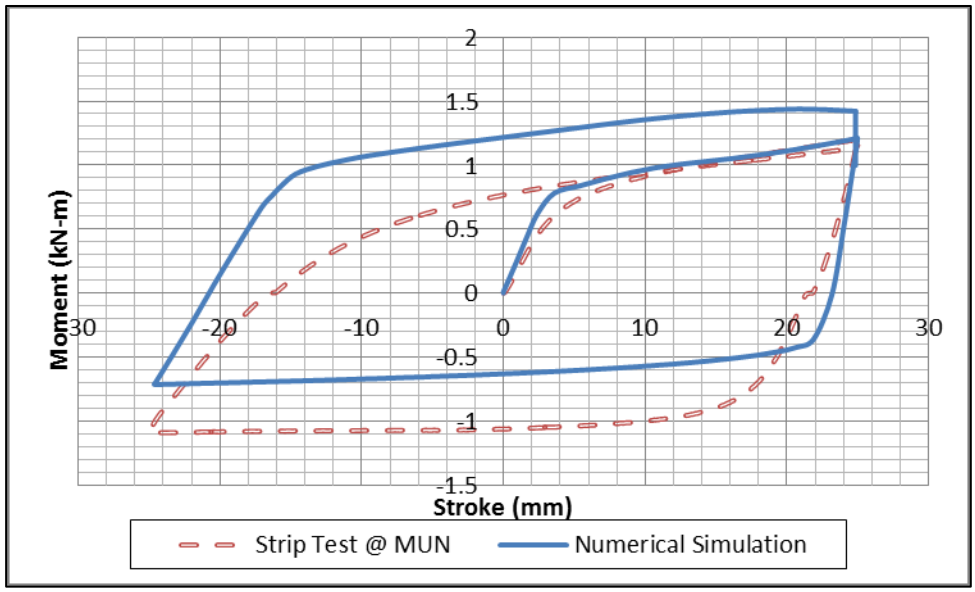

(b)

Figure 4-12: Calibration study on TR-R10-A45-S50 from this study for the (a) load-stroke and (b) moment-stroke load cycle

There is good correspondence between the peak load and peak moment for the initial one-quarter cycle, opening mode (i.e. tensile loading) of the strip coupon test. The correspondence suggests the initial damage condition for residual strain and strength properties defining the constitutive model were adequate. On subsequent loading through the hysteretic cycle, however, the isotropic hardening constitutive model, used in these numerical simulations, does not adequately capture the evolution of strength behaviour due to Bauschinger effects, kinematic hardening and damage accumulation.

A comparison between the numerical simulation and strip coupon test, based on data from Das (2003), for the load-stroke relationship and moment-stroke relationship for the first load cycle is presented in Fig. 4-13. This was conducted, as the data presented, in Das (2003), was more representative of pipe steel grade materials (X52). The results from this calibration study illustrate similar trends and requirements for future investigations.

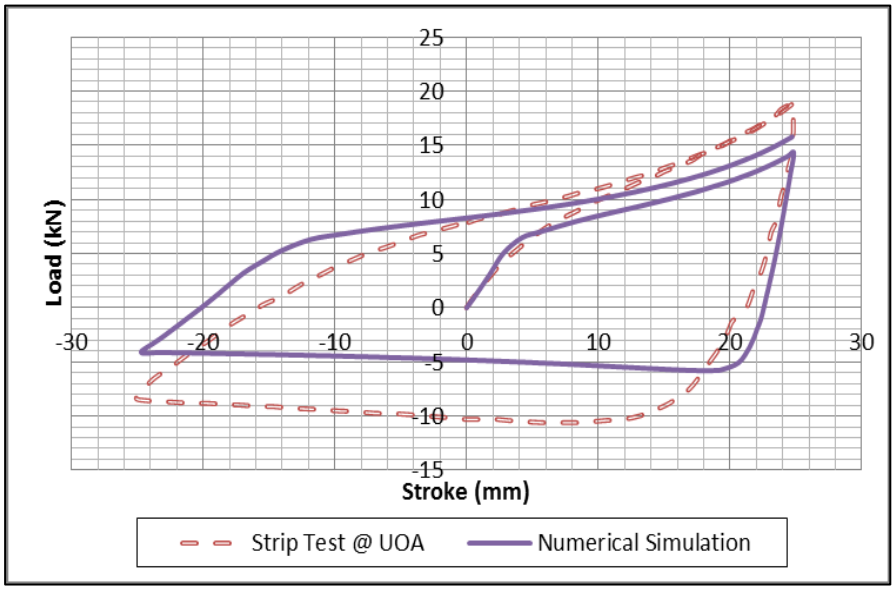

(a)

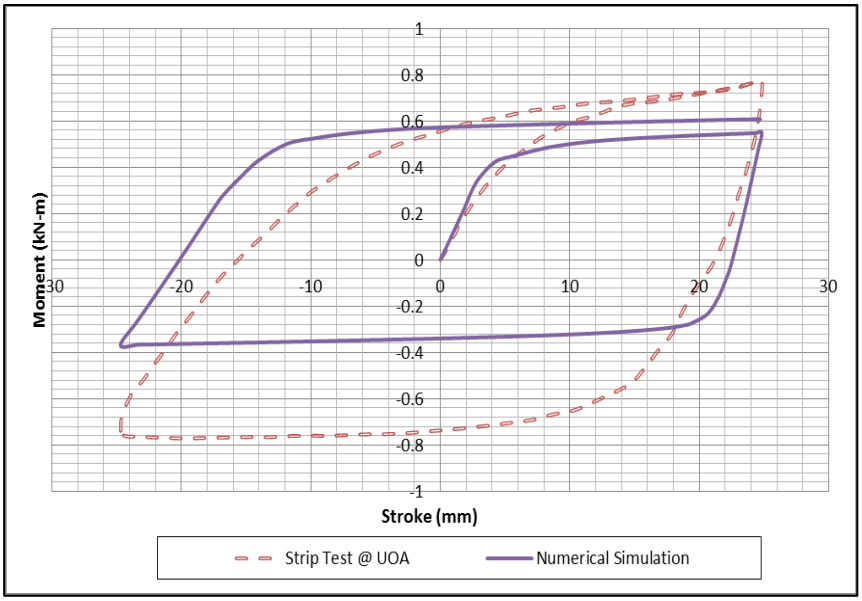

(b)

Figure 4-13: Calibration study on X52-T9-A45-R20-S50 from Das (2003) for the (a) load-stroke and (b) moment-stroke load cycle

Examination of the strain response from the physical testing indicates magnitude of the compression strain (extrados) and tension strain (intrados), for the opening mode, is approximately the same magnitude on the order of 5% to 6%. On the closing mode, however, the compression strain (intrados) on the order of 10% is greater than the tension (extrados) strain on the order of 8%.

Although the numerical modelling procedures require further refinement, it is important to note the general characteristics of the load-stroke and moment-stroke hysteretic load cycle are captured. Further experimental investigations are required to improve the constitutive model and characterize the damage accumulation. On this basis, the numerical modelling procedures can be verified with confidence for use in parameter studies to extend the knowledge bases and develop practical engineering tool for predicting the low cycle fatigue life of pipelines with local damage. Other similar studies; such as (Myrholm (2001), Das (2003), Zhang (2010)), have not conducted this calibration exercise on the strip coupon tests so it is difficult to assess the relative significance of the model uncertainty.

4.5 Conclusions and Recommendations

Experimental studies on the low cycle fatigue response of a V-shaped strip coupon, used as an analogue for pipe damage due to local buckling, was influenced by the residual strain, associated with the initial damage state due to local bending, and the incremental damage associated with strain energy during a loading cycle. The number of cycles to failure, for low cycle fatigue response, was correlated with the strain energy density

during the loading cycle. Key parameters influencing the low cycle fatigue response included residual strain, R/t, wall thickness, imposed stroke amplitude and mode of deformation (i.e. opening or closing of the strip coupon).

For lower magnitudes of initial damage state (i.e. residual strain) and strain energy density per load cycle (i.e. plastic strain increment), then a characteristic relationship was observed between strain energy density and number of cycles to failure. The response was characteristic of the Coffin-Manson type power law relationship. Lower residual strain was associated with higher R/t and lower strain energy density was associated with a lower stroke amplitude and smaller wall thickness. The experimental results are consistent with available literature on the low cycle fatigue response of pipelines with local damage. In this study, the significance of stroke amplitude (i.e. plastic strain increment) on a limiting damage accumulation response and reduced low cycle fatigue life provides new insight.

A limited calibration study with continuum finite element modelling procedures has demonstrated the simulation tool can capture the characteristic load-stroke and moment-stroke behaviour during the loading cycle. Although similar studies have been conducted, this is the first study comparing the low cycle fatigue response of V-shaped coupons using experimental and numerical methods. The numerical procedures could adequately account for the effects of coupon geometry (i.e. bend angle, R/t), material properties and residual strain effects for the first one-quarter cycle through the opening mode.

Future experimental studies should use non-invasive techniques; such as optical or thermal devices, to monitor the development of residual strain through cold work and plastic strain increments through cyclic loading. Material coupon tests are required to refine constitutive models that account for Bauschinger effects and kinematic hardening response through subsequent load cycles.

Through physical testing, using analogue and full-scale models, and numerical simulation, the adequacy of the V-shaped coupon to support the development of an engineering tool predicting the low cycle fatigue response of damaged pipelines can be evaluated. The importance of pipe diameter, pipe D/t, internal pressure, multi-axial stress state, load path, boundary conditions, and constraint effects on low cycle fatigue performance can be assessed.

4.6 Nomenclature

ϵ	Residual strain
$\Delta\varepsilon_p$	Plastic strain amplitude
δe	Change in eccentricity
A	Bend angle
b	fatigue ductility exponent
e	Eccentricity
e_o	Initial eccentricity
MUN	Memorial University of Newfoundland
N_s	No. of cycles to failure

R Coupon bend radius

S Actuator stroke

SMYS Specified minimum yield strength

t Coupon wall thickness

U_o Strain energy through hysteric loop cycle

U_o/V Strain energy density

UoA University of Alberta

UTS Ultimate tensile stress

V Volume of steel material

4.6 Acknowledgements

The authors would like to acknowledge the Wood Group Chair in Arctic and Harsh Environments Engineering at Memorial University of Newfoundland for sponsoring the research project. The opportunity to conduct the research and publish the findings of the project is greatly appreciated.

4.7 References

ABAQUS Extended Functionality HTML Documentation, Version 6.9.

Al-Showaiter, A., Taheri, F. and Kenny, S. (2011). "Effect of misalignment and weld induced residual stresses on the local buckling response of pipelines." J. PVT 133(4), 7p.

Bakhtyar, F. and Kenny, S. (2013). "Development of a fatigue life assessment tool for pipelines with local wrinkles." Proc., OMAE2013-10556:9p.

CEPA (2013). Canadian Energy Pipeline Association. http://www.cepa.com

Coffin, L.F. (1984). 84in, cycle fatigue L.Fthirty year perspective. Proc., Fatigue and Fatigue Thresholds, 3:1213-1234.

Coffin, L.F. (1954). "A study of the effects of cyclic thermal stresses on a ductile metal." eTrans. ASME, 76:931-950.

Cravero, S., Bravo, R.E. and Ernst, H.A. (2009). "Fracture mechanics evaluation of pipes subjected to combined load conditions." Proc., OMAE2009-80025 pp.219-225.

CSA Z662 (2010). Oil and Gas Pipeline Systems, 566p.

Das, S., Cheng, J.J.R., Murray, D.W., "Prediction of the fracture life of a wrinkled Steel pipe subject to low cycle fatigue load", Can. J. Civ. Eng., 34:598-607

Das, S. (2003). "Fracture of wrinkled energy pipelines." Ph.D. Thesis, University of Alberta, 252p.

DIN 2413 (1993). (Part 1 Design of steel pressure pipes). In German

Doblanko, R.M, Oswell, J.M and Hanna, A.J (2002). "Right-of-Way and Pipeline Monitoring in Permafrost - the Norman Wells Pipeline Experience."Proc., IPC-27357, 10p.

DNV RP C203 (2010). Fatigue Design of Offshore Steel Structures, 142p.

Ellyin, F. (1997). "Phenomenological approach to fatigue life prediction under uniaxial loading." Fatigue Damage, Crack Growth and Life Prediction, pp.88-90.

Fatemi, A. and Kenny, S. (2012). "Ovality of high-strength linepipes subject to combined loads." Proc., ATC, OTC-23783, 11p

Gresnigt, A.M. and Van Foeken, R.J. (2001). "Local buckling of UOE and seamless pipe." Proc., ISOPE; 2:131-142

Gresnigt, AM (1986). "Plastic design of buried steel pipelines in settlement areas," HERON; 31(4):113p.

Jayadevan, K.R., Ostby, E., and Thaulow, C. (2004). "Strain based fracture mechanics analysis of pipelines.",Proc., Int. Conf. Advances in Structural Integrity, Paper # ICAS/04-0198

Kenny, S., Barrett, J., Phillips, R. and Popescu, R. (2007). "Integrating geohazard demand and structural capacity modelling within a probabilistic design framework for offshore arctic pipelines." Proc., ISOPE2007-SBD-03, 9p.

Kibey, S.A., Minnaar, Cheng, W. and Wang, X. (2009). "Development of a physics-based approach for the prediction of strain capacity of welded pipelines." Proc., ISOPE, pp132-137.

Kibey, S., Wang, Z, Minnaar, K., Macia, M.L., Fairchild, D.P., Kan, W.C., Ford, S.J. and Newbury, B. (2010). "Tensile strain capacity equations for strain-based design of welded pipelines", Proc., IPC2010-31661, 9p.

Mahdavi, H., Kenny, S., Phillips, R. and Popescu, R. (2010). "Effect of soil restraint on the buckling response of buried pipelines." Proc., IPC2010-31617, 10p.

Mahdavi, H., Kenny, S., Phillips, R. and Popescu, R. (2012). "Significance of geotechnical loads on local buckling response of buried pipelines with respect to conventional practice." Can. Geotech. J.; 50(1):68-80.

Manson, S.S. (1966). Thermal Stress and Low-Cycle Fatigue. McGraw-Hill, 159p.

Manson, S.S. (1954). "Behaviour of materials under conditions of thermal stress." NACA TN-2933.

Michailides, D. and Deis, T. (1998). "Internal measurement and mechanical caliper technology." Proc., IPC, pp.373-378.

Morrow, J. (1965). "Thresholds, 3ts of cyclic thermal stresses on tals." orrow, J. (1965). Thresholds, 3ts of cyclic thermal stresses on tals

Myrholm, B.W. (2001) "Local buckling and fracture behaviour of line pipe under cyclic loading" M.Sc., University of Alberta,43-59, 190p.

Søtberg, T. and Bruschi, R. (1992). "Future pipeline design philosophy – Framework." Proc., OMAE 5:239-248.

Suzuki, N., Kondo, J., Ishikawa, N., Okatsu, M. and Shimamura, J. (2007). "Strain Capacity of X80 High-Strain Line Pipes." Proc., OMAE2007-29505, 9p.

Wang, S.-H., Chen, W. (2002). "A study on the pre-cyclic load-induced burst of creep deformation of a pipeline steel under subsequent static load." Materials Science & Engineering, A325:144-151

Zhang, J. (2010). "Development of LCF life prediction model for wrinkled steel pipes." Ph.D. Thesis, University of Alberta, 320p

4.8 Annex B Summary of test parameters

No.	Thickness (mm)	Radius (mm)	Angle (Degree)	Stroke (mm)	R/t (mm/mm)	Rate (mm/min)	Specimen Name
1	6.35	10	45	20	1.6	11.45	T6-R10-A45-S20
2	6.35	10	45	50	1.6	10.64	T6-R10-A45-S50
3	6.35	10	45	80	1.6	8.07	T6-R10-A45-S80
4	6.35	15	45	20	2.4	11.45	T6-R15-A45-S20
5	6.35	15	45	50	2.4	10.64	T6-R15-A45-S50
6	6.35	15	45	80	2.4	8.07	T6-R15-A45-S80
7	6.35	20	45	20	3.2	11.45	T6-R20-A45-S20
8	6.35	20	45	50	3.2	10.64	T6-R20-A45-S50
9	6.35	20	45	80	3.2	8.07	T6-R20-A45-S80
10	9.7	10	45	20	1.0	11.45	T9-R10-A45-S20
11	9.7	10	45	50	1.0	10.64	T9-R10-A45-S50
12	9.7	10	45	80	1.0	8.07	T9-R10-A45-S80
13	9.7	15	45	20	1.6	11.45	T9-R15-A45-S20
14	9.7	15	45	50	1.6	10.64	T9-R15-A45-S50
15	9.7	15	45	80	1.6	8.07	T9-R15-A45-S80
16	9.7	20	45	20	2.1	11.45	T9-R20-A45-S20
17	9.7	20	45	50	2.1	10.64	T9-R20-A45-S50
18	9.7	20	45	80	2.1	8.07	T9-R20-A45-S80
19	12.7	10	45	20	0.8	11.45	T12-R10-A45-S20
20	12.7	10	45	50	0.8	10.64	T12-R10-A45-S50
21	12.7	10	45	80	0.8	8.07	T12-R10-A45-S80
22	12.7	15	45	20	1.2	11.45	T12-R15-A45-S20
23	12.7	15	45	50	1.2	10.64	T12-R15-A45-S50
24	12.7	15	45	80	1.2	8.07	T12-R15-A45-S80
25	12.7	20	45	20	1.6	11.45	T12-R20-A45-S20
26	12.7	20	45	50	1.6	10.64	T12-R20-A45-S50
27	12.7	20	45	80	1.6	8.07	T12-R20-A45-S80

Table 4-3: Summary of Test parameters

5 CONCLUSIONS AND RECOMMENDATIONS

Localised buckling is a common form of pipeline damage which occurs because of axial forces and bending moments produced by ground movement. As a consequence to this, loss in mechanical integrity of pipeline may occur. From current and previous studies it has been concluded continuous increase of axial load after initial localised wrinkling is not detrimental to pipeline sections whereas cyclic loading leads to stress/strain concentration at wrinkle crest and due to strain reversals pipelines sections fractures within few loading cycles.

A total of 27 strip test samples were tested at the MUN facility to obtain the remaining fatigue life of the samples. A wide range of R/t from 0.8 to 3.8 was covered to increase the database. Some of the data for the experimental model is printed in Annex C.

The residual true strain showed an excellent correlation with the analytical solution for physical testing as well as the numerical analysis. With the increase in R/t the residual true strain decreases whereas for lower R/t the analytical solution diverges due to through thickness plastic material behaviour. In the numerical analysis it was observed that the residual true strain increases with the increasing thickness whereas it is constant along the width of the sample. Residual true stresses showed that von mises on the outer surface were higher than the inner surface and they were maximum at the edges on both surfaces.

Kinematic hardening parameters were defined using the tension coupon test through numerical analysis to understand the Bauschinger effect during the cyclic loading and

unloading. Parameters for kinematic hardening were defined at two points on the stress strain curve

- 0.5 % strain level (Conventional yield stress definition).
- At the onset of non-linear stress-strain behaviour.

It was observed that Bauschinger effect was not being captured when the specimen was being subjected to cyclic fatigue so other parameters such as damage accumulation needs to be defined for refinement of the numerical model.

As defined in the previous chapter hysteresis loop energy density was used as the damage parameter for this study following conclusion were drawn from the observed results.

For the load cycle, as R/t increased for constant stroke amplitude the strain energy decreased hence increasing the cycles to failure. This relationship was observed to be related to the initial damage state that was caused by the monotonic bending of the strip specimens.

It was also observed for the first load cycle the initial strain energy increased with the increase in the stroke amplitude and thickness of the specimen. Graphs (Fig 4-8 & Fig 4-10) trend for no. of cycles to failure and wall thickness and again with R/t showed consistency with the literature available in public domain.

From current studies, it was observed stroke displacement during the cyclic loading also plays in influential role in determining the remaining life of a wrinkled pipeline. An upper limit (Fig. 4-8 through Fig. 10) was also observed to exist for the maximum strain energy

density that influenced the low cycle fatigue response. Hence it was concluded that the initial damage state, strain demand per cycle and mechanical behaviour play an important role for low cycle fatigue response. Another significant factor observed was difference in relationship for remaining life and strain energy density for 20 mm stroke in comparison with 50 and 80mm strokes as discussed in chapter 4.

A characteristic relationship was observed between the strain energy density (U_o/V) and number of cycles to failure for the strip specimens, which is consistent with the previous research done by Das (2003). However, further investigation is required before developing a functional relational relationship between the damage parameters with defined coefficients.

Further investigation is required to develop a more confidence in the experimental model as the actual buried pipe is subjected to various loads and bending moment which result in wrinkle formation. Though this studies present strain energy density could be used to develop a low cycle fatigue model but other parameters such as stroke, bend radius, local plastic strain and initial damage state needs to studied as well for developing a refined model. It was observed that the difference in residual life for 20 mm stroke and 50 mm stroke were quiet abrupt so experimental testing in between these strokes needs to be carried out for refinement of the current research. Currently residual strain during the monotonic bending was measured through punch marks and residual strain was not recorded during the cyclic loading so a better procedure such as thermal imaging needs to used during the testing.

A limited calibration study for finite element modelling was also carried out, which demonstrated the numerical simulation can capture the characteristic behaviour of load stroke and moment stroke for the cyclic loading and unloading of the strip sample.

A refined constitutive material model is required for the finite element modelling which incorporates the kinematic hardening and damage parameters for developing a calibrated numerical model.

6 REFERENCES

ABAQUS Extended Functionality HTML Documentation, Version 6.9 by 3 Dassault System (3DS).

Al-Showaiter, A., Taheri, F. and Kenny, S. (2011). "Effect of misalignment and weld induced residual stresses on the local buckling response of pipelines." J. PVT 133(4), 7p.

Bai, Y., Knauf, G., Hillenbrand, H.G. (2008). "Materials and design of high strength pipelines", Proc., ISOPE,

Bakhtyar, F. and Kenny, S. (2013). "Development of a fatigue life assessment tool for pipelines with local wrinkles." Proc., OMAE2013-10556:9p.

Ballio, G. and Castiglioni, C.A., (1995). "A Unified Approach for the Design of Steel Structures under Low and/or High Cycle Fatigue." Journal of Constructional Steel Research, Vol. 34, pp41-64

Ballio, G., Calado, L., and Castiglioni, C.A. (1997). "Low Cycle Fatigue Behaviour of Structural Steel Members and Connections." Fatigue and Fracture of Engineering Materials & Structures, Vol. 20, No. 8, pp. 1129-1146.

Bouwkamp, G. and Stephen, R.M. (1973). "Large Diameter Pipe under Combined Loading." ASCE Transportation Engineering Journal, Vol. 99, No. TE3, pp. 521-536.

Bruton, D., Carr, M., Crawford, M and Poiate, E. (2005). "The safe design of hot on-bottom pipelines with lateral buckling using the design guideline developed by the SAFEBUCK Joint Industry Project." Proc., DOT, 26p.

CEPA (2013). Canadian Energy Pipeline Association. http://www.cepa.com

Coffin, L.F. (1984). 84in, cycle fatigue L.Fthirty year perspective. Proc., Fatigue and Fatigue Thresholds, 3:1213-1234.

Coffin, L.F. (1954). "A study of the effects of cyclic thermal stresses on a ductile metal." eTrans. ASME, 76:931-950.

Cravero, S., Bravo, R.E. and Ernst, H.A. (2009). "Fracture mechanics evaluation of pipes subjected to combined load conditions." Proc., OMAE2009-80025 pp.219-225.

CSA Z662 (2010). Oil and Gas Pipeline Systems, 566p.

Das, S., Cheng, J.J.R., Murray, D.W. (2007). "Prediction of the fracture life of a wrinkled Steel pipe subject to low cycle fatigue load", Can. J. Civ. Eng., 34:598-607

Das, S. (2003). “Fracture of wrinkled energy pipelines.” Ph.D. Thesis, University of Alberta, 252p

Das, S., Cheng, J.J.R., and Murray, D.W. (2002). “Fracture in Wrinkled Linepipe under Monotonic Loading.” Proceedings of the International Pipeline Conference, Sept. 30 – Oct. 3, Calgary, Canada, Vol. B, pp. 1613-1618.

Das, S., Cheng, J.J.R., Murray, D.W., and Zhou, Z.J. (2001). “Wrinkle Behavior under Cyclic Strain Reversal in NPS12 Pipe.” Proceedings of the International Conference on Offshore Mechanics and Arctic Engineering – OMAE, Jun. 3 – 8, Rio de Janeiro, Brazil, Vol. 4, pp. 129-138..

DIN 2413 (1993). (Part 1 Design of steel pressure pipes). In German

Doblanko, R.M, Oswell, J.M and Hanna, A.J (2002). “Right-of-Way and Pipeline Monitoring in Permafrost - the Norman Wells Pipeline Experience.”Proc., IPC-27357,

Dorey, A.B. (2001). Critical Buckling Strains in Energy Pipelines. Ph.D. Dissertation, Department of Civil & Environmental Engineering, University of Alberta, Edmonton, Alberta, Canada. 10p.

Dorey, A.B., Murray, D.W., Cheng, J.J.R., Grondin, G.Y. and Zhou, Z. (1999). “Testing and Experimental Results for NPS30 Line Pipe under Combined Loading” Proceedings of the International Conference on Offshore Mechanics and Arctic Engineering, OMAE, OMAE99/PIPE-5022, ASME, New York, NY, USA

DNV RP C203 (2010). Fatigue Design of Offshore Steel Structures, 142p.

DNV RP C203 (2012). Fatigue Design of Offshore Steel Structures.

Ellyin, F. (1997). “Phenomenological approach to fatigue life prediction under uniaxial loading.” Fatigue Damage, Crack Growth and Life Prediction, pp.88-90.

Fatemi, A. and Kenny, S. (2012). “Ovality of high-strength linepipes subject to combined loads.” Proc., ATC, OTC-23783, 11p

Feltner, C.E. and Morrow, J.D., (1961) “Microplastic Strain Hysteresis Energy as a Criterion for Fatigue Fracture.” Journal of Basic Engineering, 1961, pp. 18-22.

Ferreira, J., Castiglioni, C.A., Calado, L., Agatino, M.R., (1998). “Low Cycle Fatigue Strength Assessment of Cruciform Welded Joints.” Journal of Constructional Steel Research, Vol.47, pp.223-244.

Gresnigt, A.M. and Van Foeken, R.J. (2001). “Local buckling of UOE and seamless pipe.” Proc., ISOPE; 2:131-142

Gresnigt, AM (1986). "Plastic design of buried steel pipelines in settlement areas," HERON; 31(4):113p.

Halford, G.R. (1986). “Low-cycle thermal fatigue.” NASA Technical Memorandum 87225, 120p.

Jayadevan, K.R., Ostby, E., and Thaulow, C. (2004). “Strain based fracture mechanics analysis of pipelines.”,Proc., Int. Conf. Advances in Structural Integrity, Paper # ICAS/04-0198

Junak, G. and Cieśla, M. (2011). “Low-cycle fatigue of P91 and P92 steels used in the power engineering industry.” Archives of Mat. Sci & Engng, 48(1):19-24.

Kenny, S., Barrett, J., Phillips, R. and Popescu, R. (2007). “Integrating geohazard demand and structural capacity modelling within a probabilistic design framework for offshore arctic pipelines.” Proc., ISOPE2007-SBD-03, 9p.

Kibey, S.A., Minnaar, Cheng, W. and Wang, X. (2009). “Development of a physics-based approach for the prediction of strain capacity of welded pipelines.” Proc., ISOPE, pp132-137.

Kibey, S., Wang, Z, Minnaar, K., Macia, M.L., Fairchild, D.P., Kan, W.C., Ford, S.J. and Newbury, B. (2010). “Tensile strain capacity equations for strain-based design of welded pipelines”, Proc., IPC2010-31661, 9p.

Koh, S.K., and Stephens , R.I. (1991). “Mean Stress Effects on Low Cycle Fatigue for a High Strength Steel.” Fatigue of Engineering Materials and Structures, Vol.14, No. 4.pp. 413-428

Lefebvre, D., and Ellyin, F. (1984). “Cyclic Response and Inelastic Strain Energy in Low Cycle Fatigue.” International Journal of Fatigue, Vol. 6, No. 1, pp. 9-15.

Mahdavi, H., Kenny, S., Phillips, R. and Popescu, R. (2010). “Effect of soil restraint on the buckling response of buried pipelines.” Proc., IPC2010-31617, 10p.

Mahdavi, H., Kenny, S., Phillips, R. and Popescu, R. (2012). “Significance of geotechnical loads on local buckling response of buried pipelines with respect to conventional practice.” Can. Geotech. J.; 50(1):68-80.

Manson, S.S. (1966). Thermal Stress and Low-Cycle Fatigue. McGraw-Hill, 159p.

Manson, S.S. (1954). “Behaviour of materials under conditions of thermal stress.” NACA TN-2933.

Michailides, D. and Deis, T. (1998). “Internal measurement and mechanical caliper technology.” Proc., IPC, pp.373-378.

Mohareb, M. (1995). Deformational Behavior of Line Pipe. Ph.D. Dissertation, Department of Civil & Environmental Engineering, University of Alberta, Edmonton, Alberta, Canada

Mohareb, M., Alexander, S.D.B., Kulak, G.L., and Murray, D.W. (1993). "Laboratory Testing of Line Pipe to Determine Deformation Behavior." Proceedings of the 12th International Conference on OMAE, Jun. 20 – 24, Glasgow, Scotland, England, Vol. 5, pp. 109-114.

Mohareb, M., Kulak, G.L., Elwi, A., and Murray, D.W. (2001). "Testing and Analysis of Steel Pipe Segments." Journal of Transportation Engineering, Vol. 127, No. 5, pp. 408-417.

Morrow, J. (1965). "Thresholds, 3ts of cyclic thermal stresses on tals." Morrow, J. (1965). Thresholds, 3ts of cyclic thermal stresses on tals

Murray, D.W. (1997). "Local Buckling, Strain Localisation, Wrinkling and Postbuckling Response of Line Pipe"Engineering Structures, Vol. 19, No. 5, May 19997, pp. 360-371

Murray, N. W. (1993). "Stress Analysis of Wrinkle Bends in Pipelines "Thin walled structures, vol. 17, No.1, 1993, pp.65-80

Myrholm, B.W. (2001) "Local buckling and fracture behaviour of line pipe under cyclic loading" M.Sc., University of Alberta,43-59, 190p.

Nazemi, N. (2009) "Behaviour of X60 Line Pipe under Combined Axial and Transverse Loads with Internal Pressure" Ph.D. Thesis, University of Alberta

Schneider, S.P. (1998). "Flexural Capacity of Pressurized Steel Pipe." Journal of Structural Engineering, Vol.124, No.3, pp330-340.

Scotberg, T. and Bruschi, R. (1992). "Future pipeline design philosophy – Framework." In Proc., of the International Conference on Offshore Mechanics and Arctic Engineering, Calgary, Alta., 7-12 June 1992.Offshore Mechanics and Arctic Engineering (OMAE) Division of the American Society of Civil Engineers (ASME), Washington, D.C Vol 5(A) 239-248p

Souza, L.T., and Murray, D.W., (1994). "Prediction of Wrinkling Behaviour of Girth Welded line pipe", Structural Engineering Report No. 197, Department of Civil Engineering, University of Alberta, Alberta, Edmonton

Souza, L.T., and Murray, D.W. (1999). "Analysis for Wrinkling Behavior of Girth-Welded Line Pipe." Journal of Offshore Mechanics and Arctic Engineering, Vol. 121, pp. 53-61.

Sugiura, K., Chang, K.C., Lee, G.C. (1989) “Evaluation of Low Cycle Fatigue Strength of Structural Metals”, Journal of Engineering Mechanics, ASCE, 117(10): 2373-2383.

Suzuki, N., Kondo, J., Ishikawa, N., Okatsu, M. and Shimamura, J. (2007). “Strain Capacity of X80 High-Strain Line Pipes.” Proc., OMAE2007-29505, 9p.

Timoshenko, S. P. and Goodier, J.N. (1970). Theory of Elasticity , 3rd edition, Mcgraw-Hill, Newyork, N. Y.

Wang, S.-H., Chen, W. (2002). “A study on the pre-cyclic load-induced burst of creep deformation of a pipeline steel under subsequent static load.” Materials Science & Engineering, A325:144-151

Xue, L. (2008). “A unified expression for low cycle fatigue and extremely low cycle fatigue and its implication for monotonic loading.” Int. J. Fatigue 30:1691-1698.

Yao, J.T.P. and Munse, W.H. (1961). “Low-cycle fatigue of metals – Literature review.” Ship Structure Committee, U.S. Department of the Navy, Serial No. SSC-137, 37p.

Yoosef-Ghodsi, N., Kulak, G.L., and Murray, D.W. (1995). “Some Test Results for Wrinkling of Girth-Welded Line Pipe.” Proceedings of 14th Int. Conference on OMAE, Jun. 18 – 22, Copenhagen, Denmark, Vol. 5, pp. 379-388.

Zhang, J. (2010). “Development of LCF life prediction model for wrinkled steel pipes.” Ph.D. Thesis, University of Alberta, 320p

Zimmerman, T.J.E., Stephens, M.J,, DeGeer, D.D. and Chen, Q. (1995). “Compressive Strain Limits for Buried Pipelines” Proceedings of the International Conference on Offshore Mechanics and Arctic Engineering OMAE, Vol. 5 , 1995, ASME, New York, NY, USA, pp365-378

APPENDIX A

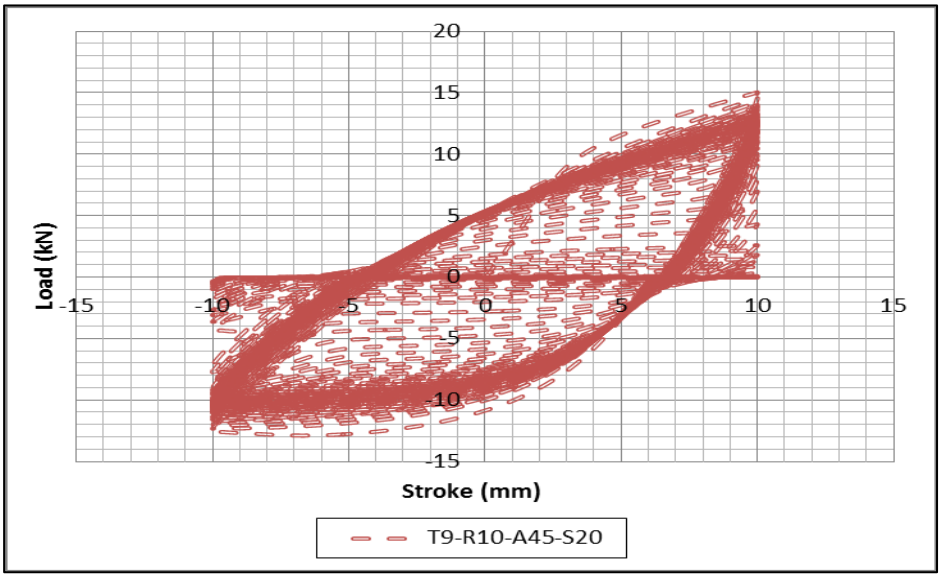

Figure A.1: Complete Load vs Stroke cycles to failure

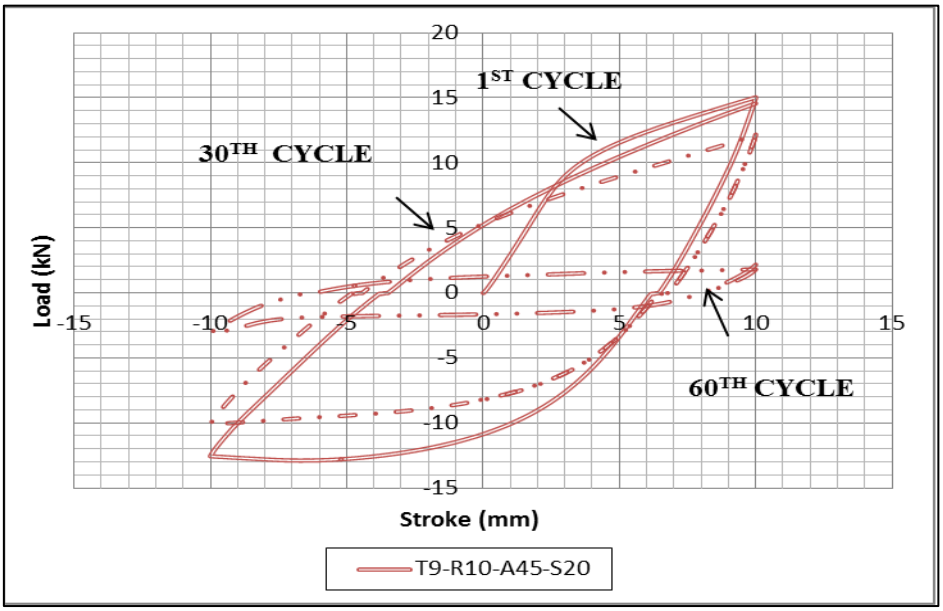

Figure A.2: Few Load vs Stroke cycles

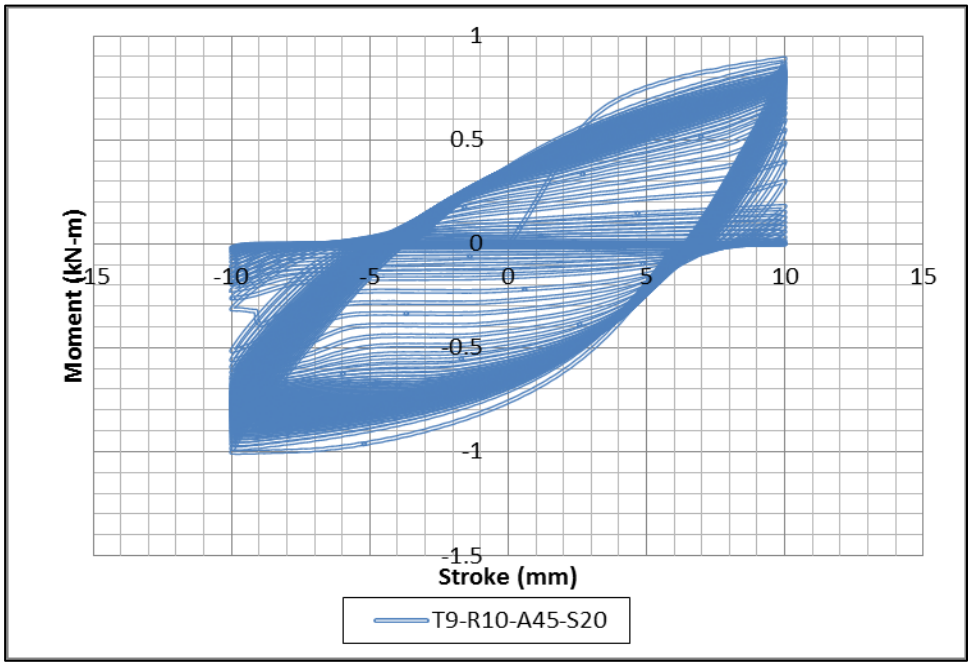

Figure A.3: Complete Moment vs Stroke cycles to failure

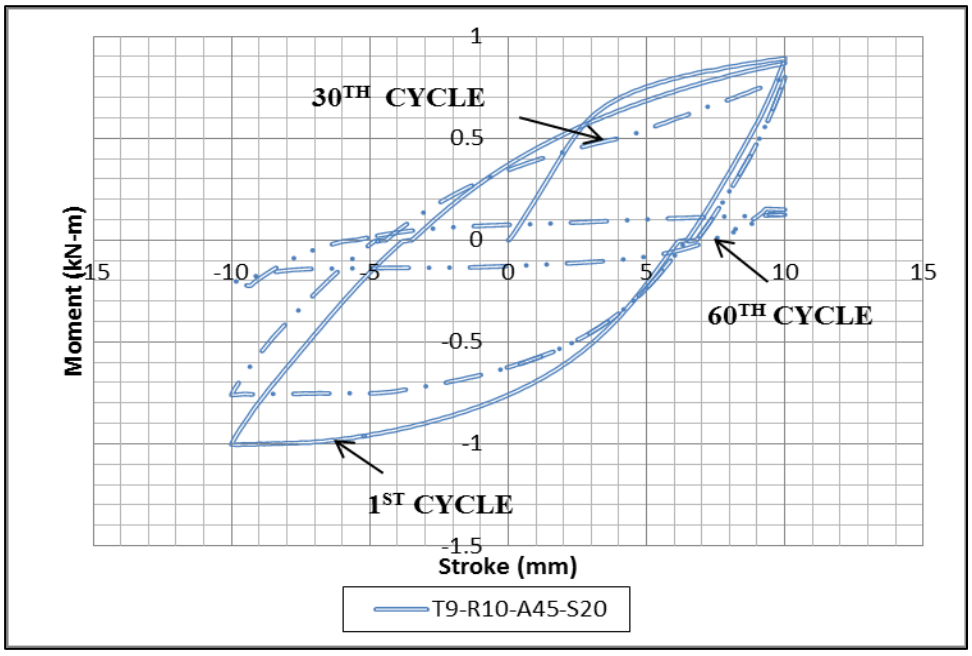

Figure A.4: Few Moment vs Stroke cycles to failure

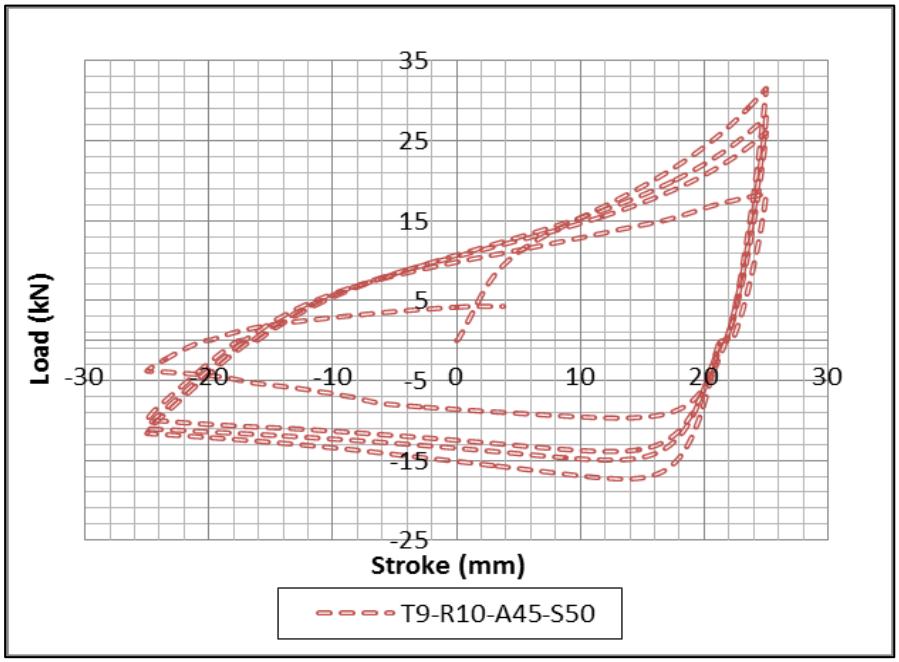

Figure A.5: Complete Load vs Stroke cycles to failure

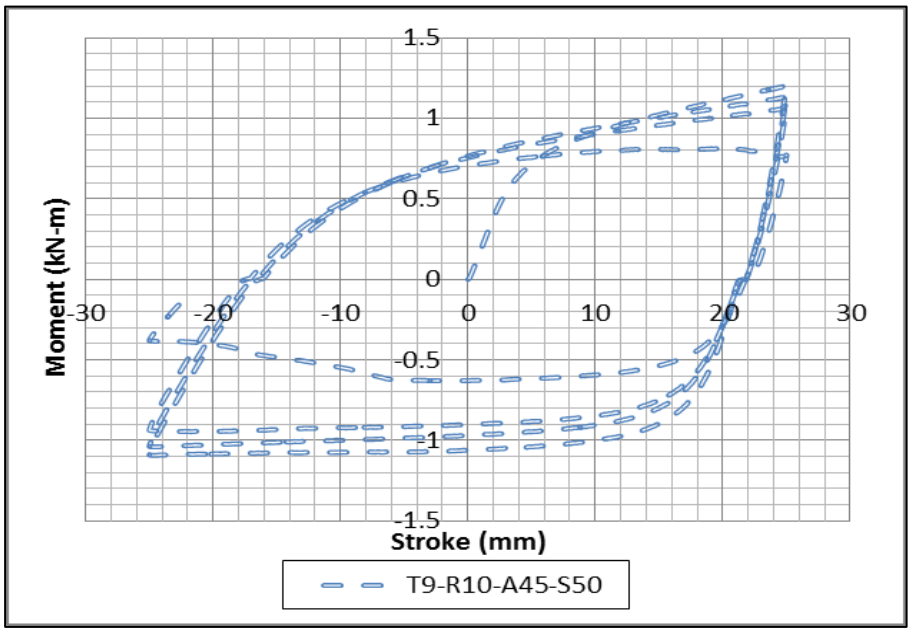

Figure A.6: Complete Moment vs Stroke cycles